WHEN LESS IS MORE: PRIMING OF SOIL ORGANIC CARBON BY PYROGENIC ORGANIC MATTER

A Dissertation Presented to the Faculty of the Graduate School of Cornell University In Partial Fulfillment of the Requirements for a Master of Science

By: Silene DeCiucies

May 2018

BIOGRAPHICAL SKETCH

Silene DeCiucies grew up in Elmore Vermont where she attended a one-room school house for grades 1-3, followed by elementary, middle, and high-school at People's Academy Public School in Morrisville, Vermont. She decided she wanted to be a soil scientist at age 16 and throughout high school and college prepared herself for this field through various academic and agricultural jobs. She attended undergraduate at Whitman College in Walla Walla, Washington where she studied geology and geochemistry and gained an appreciation for Columbia Valley wines. While attending Whitman she completed her field study at St. Andrews University in Scotland, UK. Silene began her post-graduate career at Cornell in 2014 and has spent the past three years busy in the lab, in front of a computer (which she never envisioned, but came to appreciate), teaching undergraduates, and enjoying a vast array of hobbies outside the brick confines of Bradfield Hall.

ACKNOWLEDGMENTS

This study would not be possible without the financial support from the Carbon Cycles program of USDA-DOE (NIFA 2014-67003-22069) and the NSF-Basic Research for Enabling Agricultural Development program (BREAD grant number IOS-0965336). Additional funding from the Cornell Graduate School, Soil and Crop Science Department, and Cornell Mellon Grant also contributed to the completion of this work including the travel required to run nano-SIMS samples at PNNL in Washington State. I am incredibly grateful to my major advisor Johannes Lehmann for his inspiration, support and patience throughout my sinuous journey to completion; he is a true scientist, and I cannot imagine a better academic mentor. My minor advisor Janice Thies was also incredibly instrumental in the construction of thoughts and honing of my scientific writing skills. The Picarro analyzer presented many challenges and learning opportunities, none of which could have been tackled without the dogged work of Akio Enders who was also incredibly supportive in the lab and in the majority of my growth as a scientist here at Cornell. Along with technological hurdles, the Picarro provided an endless stream of data that I could not have processed into this body of work without the help of Erika Mudrak and Stephen Parry of the Cornell Statistical Computing Department. Dominic Woolf was also incredibly helpful in processing data, and mentoring me along the way in R and in thinking like a computer. Many thanks to Kelly Hanley who was so very helpful in the lab with sample analyses, and in teaching me the ropes of Cornell campus; she was a tremendous resource throughout my time at Cornell. Thank you to Kim Sparks for her assistance with my heaps of isotope samples and complicated microbial biomass salt extracts, and to Taylor Cole and Angela Possinger for their assistance with DOC sampling. Thank you to my collaborators at PNNL, especially Odeta Qafoku and John Cliff who made the nano-SIMS analyses possible.

Above all, I would like to thank my lab group who provided endless inspiration, motivation, and knowledge in my time at Cornell. I could not have completed this work without the support and friendship of the many talented female scientists in our lab group, especially Rachel Hestrin and Leilah Krounbi who will no doubt save the world some day. Lastly, I would like to thank my friends and family who have supported me in this academic venture and in all of my other wildly distracting hobbies and life choices.

TABLE OF CONTENTS

Chapter 1
Priming mechanisms associated with pyrogenic organic matter additions to soil

Silene DeCiucies[1], Thea Whitman[2], Dominic Woolf[1], Akio Enders[1], Johannes Lehmann[1,3]*

[1]Soil and Crop Sciences, School of Integrative Plant Science, Cornell University, Ithaca, NY 14850, USA

[2]Department of Soil Science, University of Wisconsin, Madison, WI 53706, USA

[3]Atkinson Center for a Sustainable Future, Cornell University, Ithaca, NY 149850

*Corresponding author, email: CL273@cornell.edu

Keywords: Carbon sequestration, biochar, soil carbon, pyrogenic organic matter, nano-SIMS, priming

Abstract

Additions of pyrogenic organic matter (PyOM) to soil have been shown to both increase and decrease mineralization of native soil organic carbon (nSOC). This change in mineralization rate is referred to as priming, and may have important implications for carbon (C) turnover in soil. This study identifies several positive and negative priming mechanisms using high-resolution Carbon Dioxide (CO_2) measurements of a series of short-term incubation experiments with ^{13}C-labeled PyOM added to a temperate forest topsoil. Irrespective of pyrolysis temperature (200-750°C), addition of more than 2 mg PyOM g^{-1} soil significantly decreased mineralization of nSOC. Over 35 days, dilution was found to be a relevant process accounting for 20% of negative priming observed at day 7, and 13% at day 35. In comparison, substrate switching accounted for only 1.2% of negative priming at day 7 and 1.1% at day 35. Inhibition did not explain reductions in nSOC mineralization since the microbial biomass did not decrease in comparison to an unamended control. Sorption of dissolved organic carbon (DOC) from soil was responsible for the majority of negative priming observed with PyOM additions based on adsorption isotherm experiments as well as co-location of nSOC on PyOM surfaces shown by NanoSIMS. Maximum sorption potential of soil DOC was 29 times higher for PyOM pyrolyzed at 450°C than for the topsoil, and again tripled with an increase in pyrolysis temperature to 750°C. The contribution of the mechanisms mentioned above changed with time: dilution decreased after 7 days and substrate switching which initially made up less than 1% of negative priming in higher temperature PyOM could not be detected making sorption the dominant negative priming mechanism on monthly time scales. These results have long-term SOC storage implications, as sorption has longer lasting effects than substrate switching or dilution. Understanding the time-scale of sorption and potential desorption will require further long-term studies.

1.1 Introduction

Within the global carbon (C) cycle, soil organic C (SOC) represents a substantial and very active pool of likely over 2000 Pg C (Ciais et al., 2013). SOC is not only a large C pool, it is also very dynamic, being sustained by large inputs of plant litter that, under equilibrium conditions, compensate for an equally large microbial mineralization to carbon dioxide (CO_2) of about 60 Pg yr^{-1} (Ciais et al., 2013). These two factors give the SOC pool great potential in terms of its ability to affect atmospheric CO_2, since soils contain three times more C than the atmosphere or terrestrial vegetation (Stockmann et al., 2012), and small changes to SOC stocks have therefore proportionally large effects on the global C cycle.

One important avenue in which SOC pools are affected is through what is often called priming (Bingeman et al., 1953; Kuzyakov, 2010). Priming describes a change in mineralization rate through additions of organic matter, and can be positive, in that the mineralization rate of native SOC (nSOC) increases, or negative, in that the rate of mineralization decreases (Bingeman et al., 1953). Recently, the input of pyrogenic organic matter (PyOM) as a result of vegetation fires (Lehmann et al., 2008) or deliberate additions in the form of biochar (Laird, 2008) have received increasing attention with regard to priming of SOC. With climate change, forest fires are increasing globally (Abatzoglou et al., 2016), accelerating the deposition of PyOM. PyOM is already ubiquitous in soil, but its presence may increase over time (Bird et al., 2015; Santin et al., 2016), which makes priming elicited by PyOM an increasingly relevant process. Though priming by PyOM is a growing and relevant research field, why in some cases nSOC mineralization increases or decreases as a result of PyOM input is still not clear (Wang et al., 2016).

Potential mechanisms (Maestrini et al., 2015; Whitman et al., 2015) for positive priming as a result of PyOM inputs include: (i) *co-metabolism:* microbial decomposition of easily mineralizable PyOM fractions increases microbial activity, and facilitates additional decomposition of nSOC by active enzymes; (ii) *stimulation*: PyOM additions may result in improved pH, nutrient, oxygen, or water contents as well as general habitat for soil biota resulting in increased microbial activity. Negative priming may be a result of: (i) inhibition: the opposite of stimulation whereby constraints are aggravated by substrate addition, as well as by inorganic or organic substances in PyOM, which directly inhibit microbial activity. Substrate addition may also cause inhibition by interfering with the functions of enzymes or signaling compounds; (ii) *preferential substrate utilization*: easily mineralizable fractions of PyOM additions are preferentially used by microbes thus causing a decrease in nSOC mineralization; (iii) *sorption*: organic compounds are adsorbed onto PyOM surfaces, decreasing their rate of mineralization; (v) *stabilization*: greater formation of organo-mineral associations through cation bridging originating from PyOM decreases mineralization of nSOC pools; (vi) *induced aggregation*: PyOM encourages aggregation whereby C may be protected and stored for a longer period of time; (vii) *dilution*: addition of PyOM that is largely not metabolized temporarily dilutes more microbially favorable nSOC through physical dilution.

Of these stated mechanisms, several have been explored in recent studies with PyOM and SOC; dilution and substrate switching are believed to be associated with short-term priming effects through additions of easily mineralizable OM substrates (Whitman et al., 2014a), and inhibition is thought not to apply to PyOM due to the lack of observed effects on microbial biomass (Maestrini et al., 2014). Sorption has been proposed as a dominant priming mechanism in various studies (Kuzyakov et al., 2009; Cross and Sohi 2011; Zimmerman et al., 2011;

Maestrini et al., 2014; Whitman et al., 2014b) due to PyOM's high surface area, porosity, charge, and overall adsorptive nature.

Various studies have been conducted on the priming effects of PyOM on SOC, yielding a wide array of responses (Maestrini et al., 2015; Whitman et al., 2015; Wang et al., 2016), and emphasize the need for mechanistic studies that can help in understanding priming mechanisms within different environments. Microbial biomass and activity often increase after additions of PyOM (Lehmann et al., 2011) indicating that direct microbial toxicity is unlikely to play a role. Yet such changes may still either reduce nSOC mineralization by substrate switching or increase nSOC mineralization by co-metabolism, the net effect being uncertain. It is clear that soil type (Luo et al., 2011; Keith et al., 2011), nSOC properties (Cross and Sohi, 2011; Whitman et al., 2014b), soil temperature (Fang et al., 2015) and the presence of plants (Whitman et al., 2014b; Keith et al., 2015; Weng et al., 2017) play important roles. While many of these studies had a limited ability to comprehensively identify mechanisms, it is clear that different PyOM properties have significant effects on priming that may even change over short periods of time (Zimmerman et al., 2011). Many of the changes in nSOC mineralization induced by priming occur over periods of weeks to months (Wardle et al., 2008; Zimmerman et al., 2011; Whitman et al., 2014ab) and likely involve several mechanisms operating simultaneously with changing intensity over time. A comprehensive assessment of priming effects by PyOM with high temporal resolution that would allow attribution of the different mechanisms has not been done.

This study investigates key mechanisms of priming by additions of PyOM. Specifically, the objectives include (1) simultaneous assessment of the contributions by positive and negative priming including inhibition (by toxicity), substrate switching, dilution, co-metabolism, and adsorption; (2) quantification of the rapid temporal changes in priming mechanisms operating

during the period immediately following OM input to soil; (3) assessment of temporal changes of priming mechanisms over the course of several months.

We hypothesized that (i) dilution is not a significant mechanism in causing negative priming, and is restricted to short time scales; (ii) inhibition by direct OM toxicity is not a significant mechanism for priming; (iii) substrate switching or co-metabolism are not quantitatively important mechanisms in response to PyOM additions; and (iv) sorption is the most effective negative priming mechanism for PyOM.

1.2. Materials and Methods

1.2.1 Biomass production

Two sets of Preble shrub willow (*Salix viminalis x S. miyabeana*) were grown concurrently, one in ambient CO_2 greenhouse conditions, and one in an isotopically enriched $^{13}CO_2$ growth chamber. Natural abundance willow was grown to provide a near-identical product that could be used to dilute the valuable labeled material to be used for some analytics. Both sets were grown in Cornell potting mix from 0.3 m willow cuttings obtained from Cornell's Willow Research Farm in Geneva, NY and were watered every other day and fertilized weekly. The enriched $^{13}CO_2$ willow was grown in a Percival AR 100L3 CO_2 controlled growth chamber (Percival, Perry, IA, USA). The plants were subjected to an 18-hour photoperiod at 24°C, and 6 hours of darkness at 17°C. Humidity was maintained using a de-humidifier and, during the photoperiod, CO_2 levels were kept at 400 ppm. The plants were fertilized with a modified Hoagland Solution (Whitman et al., 2014a) in which N was supplied in the form of ^{15}N-ammonium sulfate (10 atom%). Once first buds emerged from the willow cuttings, $^{13}CO_2$ was provided to the plants.

Over the course of their 6 months of growth, 20 L of 99 atom% ^{13}C-CO_2 was supplied at an increasing rate throughout the growth period. In order to deliver the gas, a plastic CO_2-impermeable bag was filled with CO_2 and attached to 1-mm nylon tubing which delivered the gas though a solenoid peristaltic pump into the growth chamber. This allowed a slow steady supply of CO_2 for 14 of the 16 hours in the photoperiod. Willow was harvested 3 times throughout the 6-month growing period. At each of the three harvests, all of the new growth was removed from the stem with the exception of 2-3 nodes which were left for re-growth. The plants were harvested before they reached reproductive maturity at each of the three harvests. The plant material was separated into stems and leaves, and oven dried at 70°C.

1.2.2 PyOM production

Oven-dried willow stems were milled to <2 mm using a hammer mill and pyrolyzed in a modified muffle furnace under Ar gas using a 2.5°C min^{-1} ramp rate and 30 min dwell time at 200, 300, 450, 600, and 750°C. The PyOM was cooled slowly under Ar. To prepare for incubations, PyOM was shaken in deionized (DI) water overnight and rinsed to remove easily-soluble ash and water soluble material. All PyOM was pH adjusted to the pH of the soil used in the incubation (4.89) over the course of several days using 1 M HCl. Once the target pH was reached, PyOM was rinsed, oven dried at 70°C and sieved to 150-850 μm. PyOM was assessed for ash, volatiles, and fixed carbon according to Enders et al. (2012). Nitrate (NO_3^-) and ammonium (NH_4^+) were extracted with 2M KCl and quantified on a continuous flow analyzer (Bran and Luebbe Autoanalyzer, SPX, Charlotte, NC). Dissolved organic carbon (DOC) was assessed by water extraction using a 1:20 (w/v) ratio, shaken for 1 hour, filtered, and run on a

DOC analyzer (Shimadzu TOC-5000A, Columbia, MD, USA). Total C, nitrogen (N), hydrogen (H), and oxygen (O), bulk $\delta^{13}C$ and $\delta^{15}N$ were measured using a Delta V Isotope Ratio Mass Spectrometer (Thermo Scientific, Germany) coupled to a dry combustion analyzer (Carlo Erba NC2500 Elemental Analyzer, Italy). PyOM was digested in a combination of nitric acid (HNO_3) and hydrogen peroxide (H_2O_2) and analyzed using Inductively Coupled Plasma Optical Emission Spectrometry (ICP-OES) for principal components. Cation exchange capacity (CEC) was determined using Graber et al. (2017), and pH was determined in DI water using a glass electrode (detection limit of 0.01 pH units) with a PyOM:water ratio of 1:10 (w/v) (Orion 3-Star pH Benchtop; Thermo Electron Corporation, Beverly, MA, USA). Specific surface area (SSA) was quantified using the B.E.T. method with CO_2 at 273.15 K and N_2 at 77.039 K (ASAP 2020, Micromeritics, Atlanta, GA, USA). Uncharred biomass was analyzed using the same techniques as described above.

Table 1. Properties of PyOM and the original uncharred biomass.

Property (units)	Biomass	PyOM				
		200°C	300°C	450°C	600°C	750°C
Ash (%)	0.63	0.00	1.63	1.87	2.92	2.72
Volatiles (%)	92.52	86.90	49.17	23.86	13.99	10.48
Fixed carbon (%)	6.85	13.51	49.20	74.27	83.09	86.80
Initial pH (H_2O)	5.38	5.84	9.57	10.77	12.13	12.64
Extractable NO_3 and NO_2 (mg NO_3+NO_2-N kg^{-1})	11.60	9.96	1.02	1.06	0.88	0.64
Extractable NH_4 (mg NH_4-N kg^{-1})	106.84	19.80	12.15	15.12	6.18	6.32
Water extractable C (DOC) (mg kg^{-1})	5776.0	2343.9	478.7	275.4	75.8	102.5
Total H (%)	6.91	10.27	5.13	3.17	2.00	1.00
Total O (%)	47.84	72.63	21.79	12.78	9.23	7.22
Total C (%)	56.02	46.02	67.21	76.49	80.67	81.83
Inorganic C (%)	0.00	0.00	0.00	0.00	0.00	0.00
Total N (%)	1.77	1.60	2.91	3.05	2.64	2.60
Total P (mg kg^{-1})	338.2	242.0	981.7	1965.1	2821.0	3050.9
C/N (w/w)	31.6	28.9	23.1	25.1	30.6	31.47
$H/C_{organic}$ (molar)	1.47	2.67	0.91	0.50	0.30	0.15
$O/C_{organic}$ (molar)	0.64	1.18	0.24	0.13	0.09	0.07
Bulk ^{15}N (atom %)	8.19	7.81	8.07	7.95	8.00	8.02
Bulk $\delta^{13}C$ (‰)	748.11	755.66	749.04	693.56	749.85	749.85

1.2.3 Preparation of additional amendments

Quartz sand (150-200 μm, U.S. Silica, Frederick, MD, USA), perlite, (Lambert, Quebec, CA) and temperate subsoil (B-horizon of soil used in incubation) were sieved to 150 -850 μm and ashed in a modified muffle furnace for 8 hours at 500°C to be used in the dilution incubation experiment.

1.2.4 Soils

Soil was collected from a mixed deciduous forest on Mt. Pleasant in Dryden, NY. The soil is a Mardin channery silt loam- a coarse loamy, mixed, active, mesic typic Fragiudept that has had no instance of burning in recorded history. For this set of incubations, the topsoil (0.02-0.2 m) horizon was collected after removing the O-horizon material. Field capacity of each soil mixture (soil+amendment) was determined (method modified from Black et al., 1965) in PVC tubes having the exact diameter of the 60 mL qorpax jar used in the incubations. Particle size fractionation and texture analysis was done according to Kettler et al. (2001). NO_3^- and NH_4^+, total C, N, H, and O, bulk $\delta^{13}C$ and $\delta^{15}N$, pH, and total nutrient contents were measured as described above for PyOM. Water soluble C (DOC) was extracted in DI H_2O using a 1:10 ratio (w/v), shaken for 1 hour, filtered, and analyzed using the same method as PyOM. SSA was quantified using the B.E.T. method with N_2 at 77.039 K (ASAP 2020, Micromeritics, Atlanta, GA, USA), and inorganic C was assessed using the Bernard calcimeter gas displacement method (Nelson, 1996).

Table 2. Properties of the studied soil.

Property (units)	Temperate Mardin Topsoil
Sand (%)	15.9
Silt (%)	59.5
Clay (%)	24.6
Texture	Silt loam
Field capacity (mL g^{-1} soil)	0.82
Extractable NO_3^- and NO_2^- (mg NO_3+NO_2-N kg^{-1})	3.99
Extractable NH_4^+ (mg NH_4-N kg^{-1})	45.7
Water-extractable C (DOC) (mg kg^{-1})	704
Total C (%)	5.28
Total N (%)	0.38
Total P (mg kg^{-1})	14.9
Bulk $\delta^{13}C$ (‰)	-27.4
Bulk $\delta^{15}N$ (‰)	1.22
C:N (g g^{-1})	13.90
pH (H_2O)	4.89

1.2.5 Incubation experiments

All incubations took place in 1-L mason jars. Thirty mL DI water was poured in the bottom of each jar to maintain 100% humidity and each jar contained a smaller 60-mL qorpax bottle that contained 40 g wet soil+amendment mixture. Dry topsoil and dry amendments were added to the bottles, mixed, and water was added to achieve 65% field capacity for the soil+amendment mixture. One mL of a modified Hoagland solution was added to each jar to supply sufficient nutrients to exclude any effects of nutrients added with amendments (Whitman et al., 2014b). A control treatment with no PyOM was also included for each incubation. Each treatment was replicated 5 times. Incubations were continuously monitored using a Picarro CO_2 stable isotope analyzer (G2201-I, Santa Clara, CA, USA) fitted with a custom-built manifold capable of sampling 112 Mason jars. Each sample jar was measured for 6 min during each sampling period, and subsequently purged with CO_2-free air. Data were collected at a rate of two measurements s^{-1} over the 6-min sampling period, and also throughout the 6-min sample purge in order to record the baseline values before each cycle's respiration.

Experiment 1: Volumetric dilution

The PyOM was added to soil at 5 mg g^{-1} in comparison to different bulking amendments to assess the effect of dilution on SOC mineralization. Ashed subsoil, perlite, and quartz sand, were added to soil at an equivalent volume to the PyOM addition (1.36 cm^3 jar^{-1}) in order to simulate the same amount of physical dilution (see supplementary online Table S1). Each treatment was replicated five times. The samples were incubated for 35 d and were measured for CO_2 and its isotope content 84 times over the duration of the incubation.

Experiment 2: Pyrolysis temperature

The PyOM produced at different temperatures (200, 300, 450, 600, 750°C) was added to soil at a rate of 10 mg g^{-1}. Each treatment was replicated five times. The samples were incubated for 62 d and sampled daily.

Experiment 3: Application rate

The PyOM was added to soil at rates of 0 (control), 0.5, 1, 2.5, 5, and 10 mg g^{-1} dry soil. Each treatment was replicated five times. The samples were incubated for 35 days and sampled daily for CO_2 and its isotope content.

1.2.6 Adsorption isotherms

The DOC for the adsorption experiment was obtained by shaking the soil in DI water for 2 h, then centrifuging and filtering the soil slurry through a 0.45-µm glass fiber filter (GC-50, Advantec, Tokyo, Japan). The DOC was diluted to 7 concentrations (0, 10, 20, 50, 80 100 and 160 mg g^{-1}) and each dilution was shaken with 0.5 g adsorbent (PyOM or soil) for 12 h before centrifugation (2000 rpm for 10 min), filtration, and analysis. Filtrates and original DOC extracts were analyzed using a Shimadzu TOC analyzer (Shimadzu TOC-5000A,Columbia, MD, USA).

1.2.7 Microbial biomass

Upon conclusion of the incubation, samples were immediately assayed for microbial biomass with simultaneous chloroform ($CHCl_3$) using a modified method of Witt et al. (2000). The extracts were dried at 50°C and analyzed for isotopic C concentrations using the modified method from Bruuslema et al. (1996). Dried salt extracts were analyzed for total C and $\delta^{13}C$ using a Delta V Isotope Ratio Mass Spectrometer (Thermo Scientific, Germany) coupled to a Carlo Erba NC2500 Elemental Analyzer (Italy). An extraction efficiency coefficient of 0.45 was used to determine the total microbial biomass (Vance et al., 1987; Jenkinson et al., 2004), and a 2-part partitioning equation was used to attribute the microbial biomass C (MB-C) source to either nSOC or PyOM. After microbial biomass extraction, soils were air-dried and sealed in air-tight storage bottles.

1.2.8 NanoSIMS

NanoSIMS images were collected at the Environmental Molecular Sciences Laboratory at the Pacific Northwest National Laboratory in Richland, WA, USA. To prepare samples for NanoSIMS analyses, air-dried intact micro-aggregates (100-400 μm) were broken in half to expose an interior fresh surface, and depending on the area of interest, either a PyOM particle was removed, or the entire aggregate was used once the back had been sliced off. Two methods for sample preparation were included to reduce biases and results allowed identical conclusions: (a) The sample was pressed into indium foil using a glass microscope slide. (b) Samples were embedded in Field's metal (ESPI Metals, Ashland, OR, USA) by dropping the sample into melted metal at 60°C and quickly covering it with a glass microscope slide so that the top of the

sample and Field's metal were completely flat. Samples were then sputter coated in ~5 μm high purity iridium to improve conductivity and imaged with a scanning electron microscope to determine regions of interest which were mapped. The samples were measured using NanoSIMS (Cameca NanoSIMS 50L spectrometer, AMETEK Inc., CAMECA SAS, Paris, France). Negative secondary ions were accelerated to 8 keV and were simultaneously counted using electron multipliers (EM)s. The magnetic field was stabilized using NMR regulation and secondary ion peaks were monitored throughout the day and adjusted for drift. Prior to image analysis, image areas were pre-sputtered with about 2×10^{16} ions cm^{-2}. Ion images of $^{12}C_2^-$, $^{12}C^{13}C^-$, $^{12}C^{14}N^-$, $^{12}C^{15}N^-$, $^{28}Si^-$, $^{31}P^-$, and $^{32}S^-$were collected using a 1.5 pA, primary beam that had a diameter of approximately 120 nm and a dwell time of 13.5 ms $pixel^{-1}$. Each 45μm × 45μm image consisted of two – 256 × 256 pixel frames.

Images were processed using ImageJ software with the open-MIMS plug-in for Fiji (nano.bwh.harvard.edu/MIMSsoftware). Images were corrected for deadtime and QSA (β=0.5) pixel by pixel and frame-aligned prior to summing the frames. Isotope images were calculated as $^{12}C^{13}C/^{12}C_2$ and $^{12}C^{15}N/^{12}C^{14}N$ and expressed relative to VPDB as $\delta^{13}C$ (‰), or relative to air as $\delta^{15}N$ (‰). An in-house yeast reference material with known $\delta^{13}C$ (-11‰) and $\delta^{15}N$ (+0.4‰) (James Moran, PNNL, Personal communication) was analyzed during each analytical session to ensure quality control and to calibrate isotope analyses of the biochar.

1.2.9 Data analysis

Langmuir isotherms were fitted to the adsorption data using the following equation:

$qe = Q_O * K_L * C_e / (1 + K_L * C_e)$

whereby Qe (mg DOC L^{-1}) is the adsorption capacity, C_e (mg DOC L^{-1}) is the equilibrium concentration after adsorption, Q_o (mg DOC g^{-1}) is the maximum sorption capacity of the amendment, and K_L (L mg^{-1}) is a Langmuir constant. Calculations were performed using non-linear regression, and sum of squares (r^2) were calculated using SigmaPlot 12.5 (SAS, Cary, NC).

Respiration data were analyzed using R version 3.3.1 (R Foundation for Statistical Computing, Vienna, Austria). Sample respiration was parsed into PyOM and nSOC-derived CO_2-C using the following equation:

$\delta_{measured} = \delta_{nSOC} * (f_{nSOC}) + \delta_{PyOM} * (1\text{-}f_{nSOC})$

$f_{nSOC} = \delta_{measured} - \delta_{PyOM} / \delta_{nSOC} - \delta_{PyOM}$

$f_{nSOC} * CO_2$-C respired = respired nSOC

Isotopic content of bulk PyOM (δ_{PyOM}) was used as endmember to be used in isotope partitioning equations, as bulk PyOM values were shown to be appropriate proxies for $^{13}CO_2$ from PyOM (Whitman et al., 2014b). Soil isotope values (δ_{soil}) to be used in isotope partitioning equations were obtained daily using the average isotope content for CO_2 from control treatments with no added labeled material. Differences were assessed using ANOVA analysis and Tukey corrections for multiple comparisons, as well as two-sample t-tests between individual treatments. Cumulative respiration data were analyzed using pairwise comparisons between treatments based

on a mixed effects linear model with a random effect on the sample jar to correct for multiple samplings.

1.3. Results

1.3.1 nSOC mineralization

In comparison to other bulking materials with the same volume, adding PyOM or ashed subsoil caused significant and rapid reduction in nSOC mineralization (Fig. 1a) and greater cumulative negative priming after day 10, with PyOM additions showing more negative priming than ashed subsoil by day 50 (Fig. 1c). Cumulative nSOC mineralization after perlite addition was significantly lowered only by day 50 ($p < 0.05$), and reductions after sand additions were not significant during the entire observation period. Most of the changes occurred during the first five days, except after additions of PyOM which resulted in slower but continuously increasing negative priming over time (Fig. 1c).

Adding PyOM caused a reduction in nSOC mineralization by 0.72 mg CO_2-C g^{-1} soil, in comparison to PyOM mineralization of only 0.0076 mg CO_2-C g^{-1} soil (Fig. 1d), which accounts for only 1% of the negative priming observed.

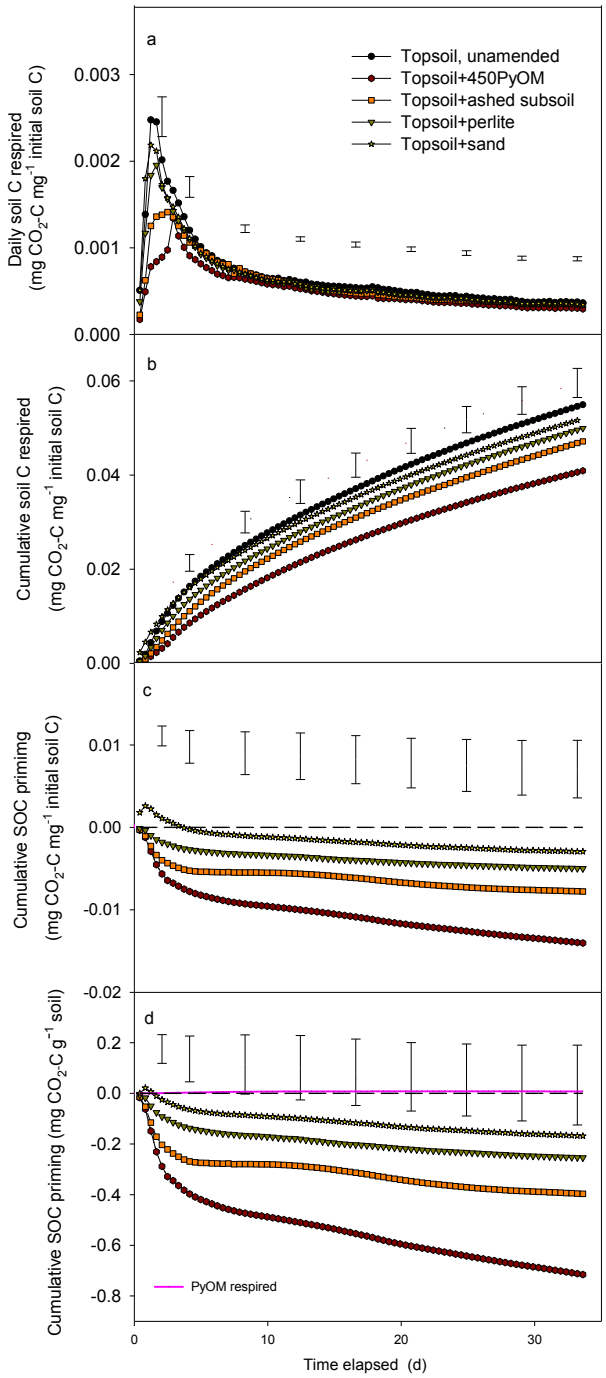

Fig. 1. Mineralization of nSOC and PyOM after additions of either PyOM, quartz sand, perlite or ashed subsoil. a. Mean daily nSOC respired per unit initial C per day, error bars indicate LSD at that timepoint. b. Mean cumulative nSOC respired per unit initial C. c. Mean cumulative nSOC priming per unit initial soil mass C. Cumulative priming calculated by subtracting unamended control from treatment value. Dashed line represents unamended soil, data above this line indicate positive priming, below indicate negative priming. d. Mean cumulative nSOC priming per unit soil mass. Dashed line represents unamended soil, pink solid line indicates PyOM-C respired g^{-1} soil (n=5; bars show LSD at $p<0.05$).

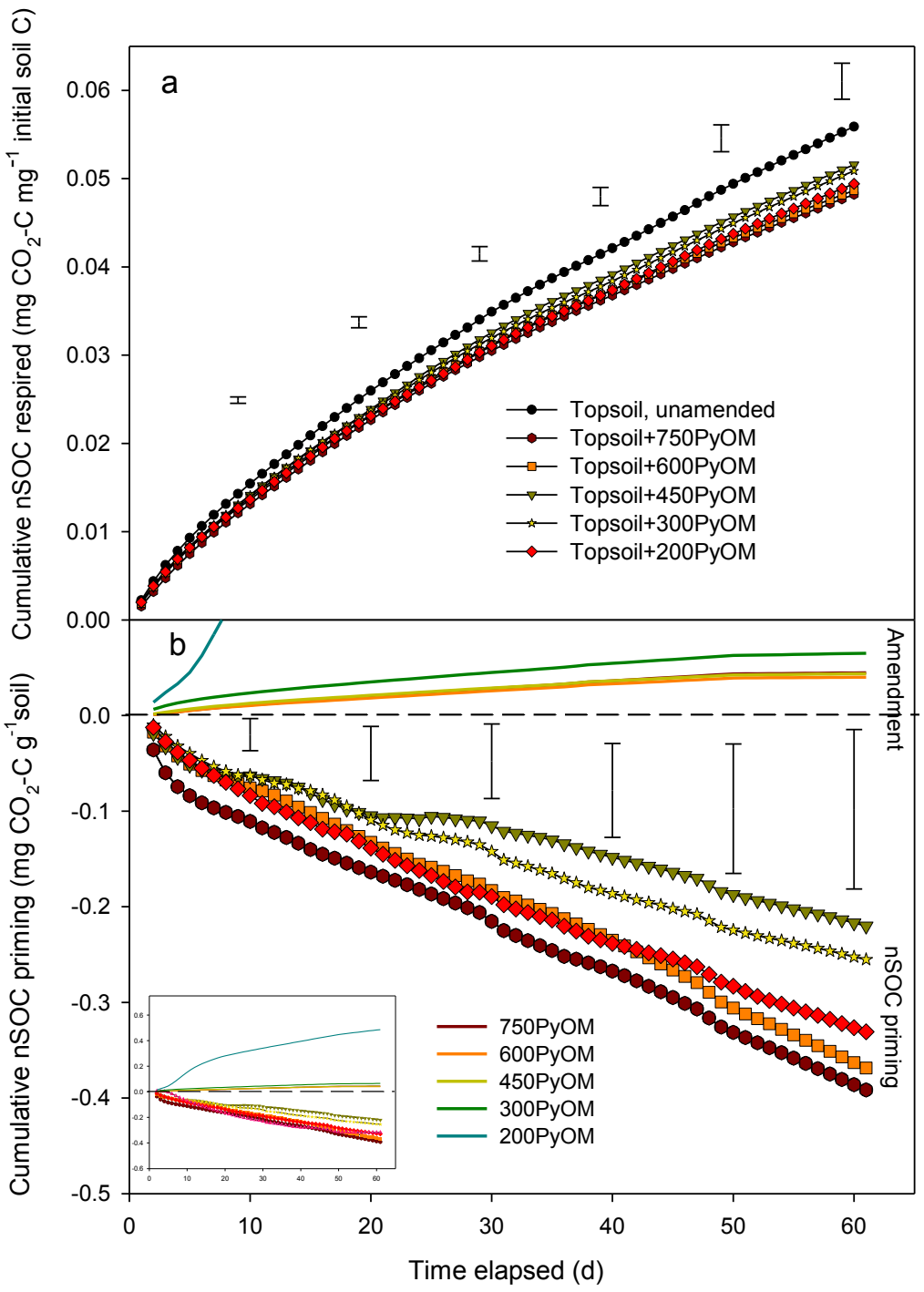

Fig. 2. Cumulative nSOC mineralization after additions of PyOM pyrolyzed at different temperatures. a. Mean cumulative nSOC respiration per unit initial soil C. b. Mean cumulative priming per unit soil determined by subtracting unamended control from treatment value. Dashed line represents unamended soil. Solid lines indicate PyOM-C respired. Inset image shows entire range of data (n=5; bars indicate LSD at $p<0.05$).

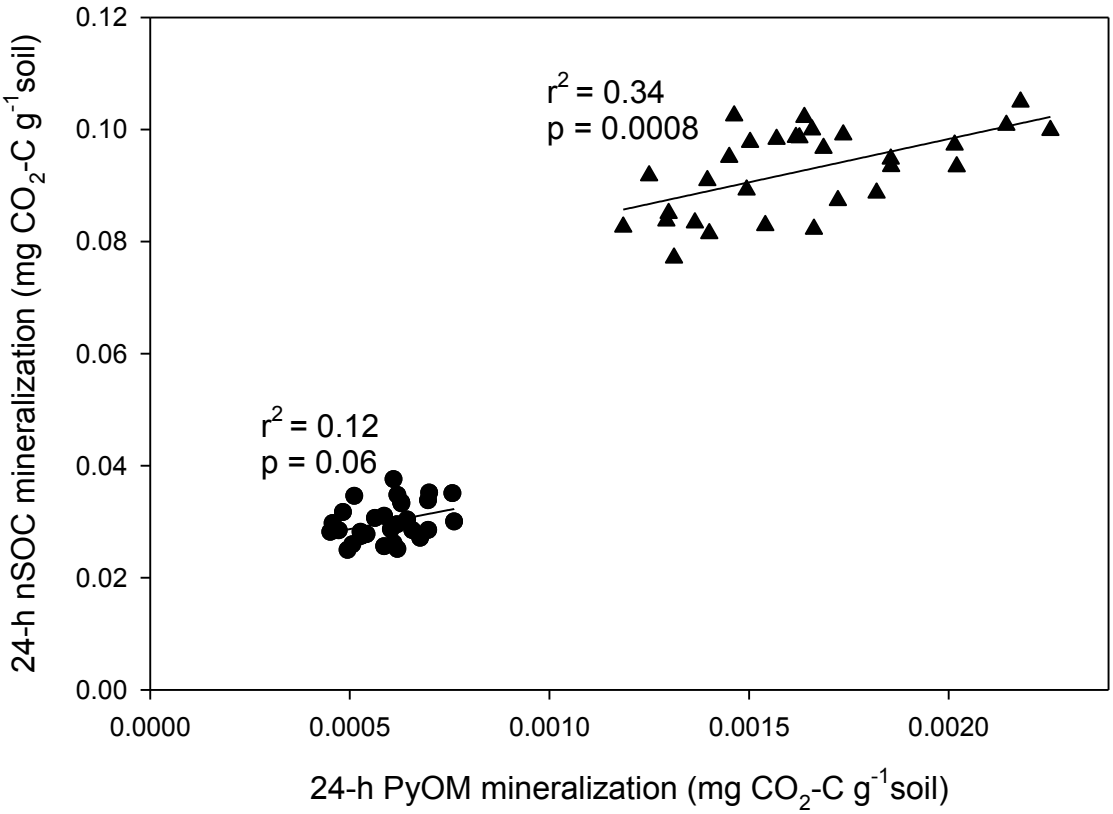

Fig. 3. Mineralization of nSOC over 24 h plotted against PyOM mineralization over the same time period at day 3 (triangles) and day 40 (circles) of Experiment 2 shown in Fig. 2. PyOM produced at 300, 450, 600 and 750°C included in regression (n=5).

All PyOM materials irrespective of pyrolysis temperature (200-750°C), as well as uncharred biomass caused negative priming (Fig. 2a). PyOM pyrolyzed at 750°C caused the most negative priming (different from control at day 30) followed by those at 600, 200, 300 and 450°C at days 30, 30, 40, 50, and 60, respectively. Adding 750PyOM resulted in 17% lower cumulative nSOC mineralization at day 60 than the control.

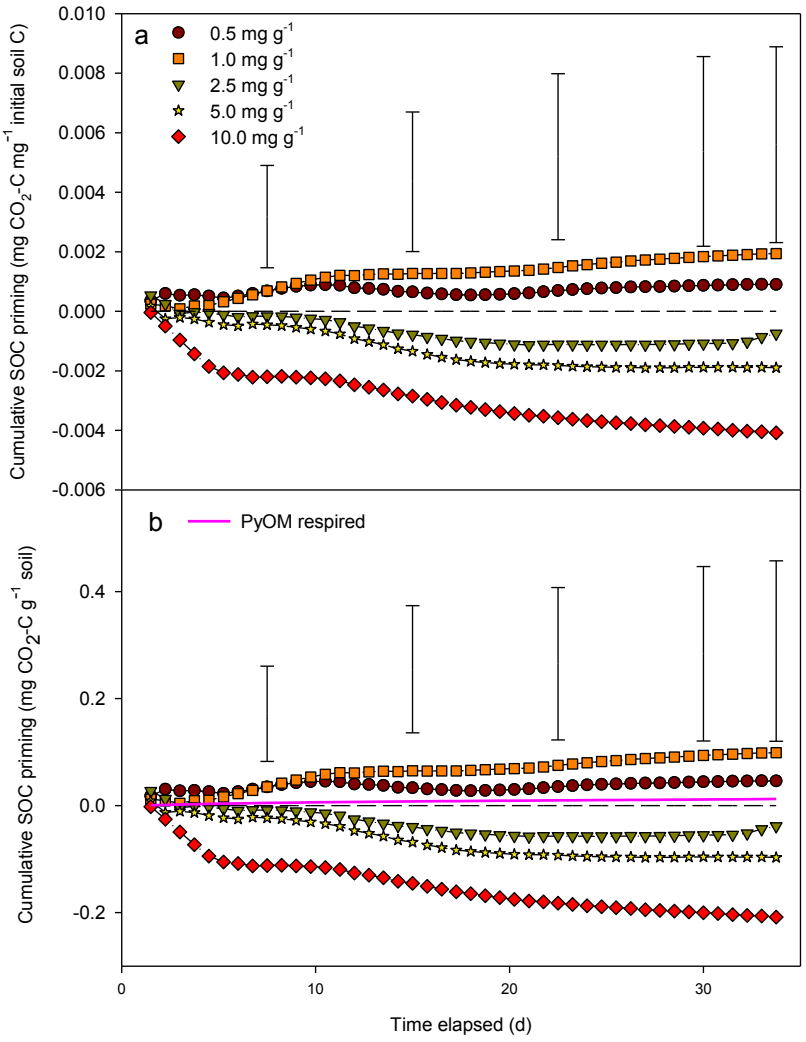

Fig. 4. Cumulative nSOC priming after additions of different rates of PyOM (produced at 450°C), a. per unit initial soil C d^{-1}, or b. g^{-1} soil per day. Dashed horizontal line represents unamended soil. Solid line indicates PyOM-C respiration g^{-1} soil for an application rate of 10 mg g^{-1} (n=5; bars indicate LSD at $p<0.05$).

Increasing the application rate significantly changed cumulative nSOC mineralization (main effect $p<0.05$). Only PyOM application rates of 10 mg g^{-1} significantly ($p<0.1$) decreased cumulative nSOC mineralization by 10% at day 35 as compared to the PyOM addition of 1.0 mg g^{-1} ($p<0.05$) (Fig. 4)

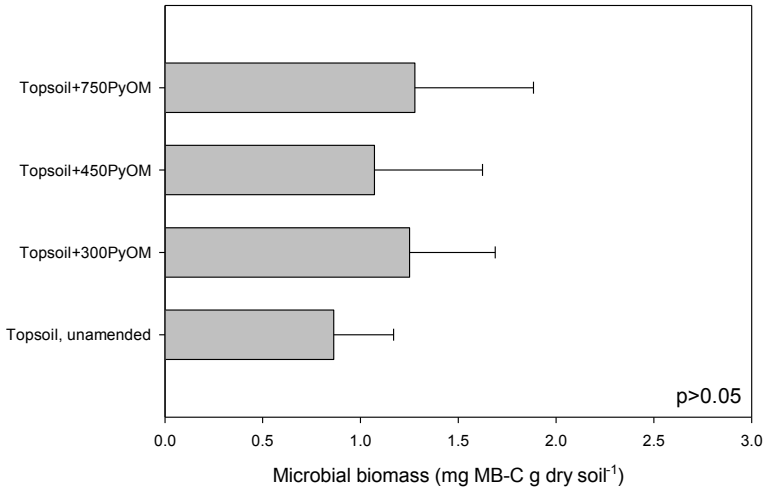

Fig. 5. Microbial biomass (MB) for experiment 2 (means and standard errors; n=5).

1.3.2 Microbial biomass

Microbial biomass did not vary between amendments (Fig. 5).

1.3.3 Adsorption of dissolved organic carbon

PyOM produced at 750°C adsorbed about three times more DOC than that produced at 450°C , the latter causing a maximum adsorption 19 times greater than either soil (Fig. 6; Table 4). PyOM pyrolyzed at 200°C did not adsorb any DOC but rather released DOC into solution.

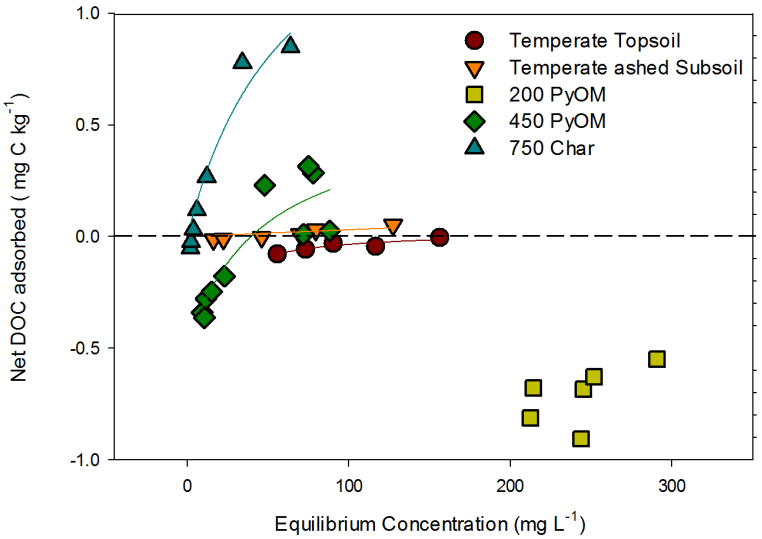

Fig. 6. Adsorption of DOC by PyOM pyrolyzed at 200, 450 and 750°C in comparison to topsoil and ashed subsoil (n=1).

Table 4. Adsorption maximum, Langmuir constant and regression values for DOC adsorption to topsoil, ashed subsoil, and PyOM pyrolyzed at either 450 or 750°C.

	Q_O (mg DOC L^{-1})	K_L (L mg^{-1})	r^2	p-value
Topsoil	0.02	0.160	0.84	0.0280
Ashed subsoil	0.03	0.470	0.66	0.0497
450PyOM	0.57	0.024	0.79	0.0005
750PyOM	1.80	0.016	0.94	0.0600

1.3.4 NanoSIMS

Labeled PyOM showed a strong ^{13}C and ^{15}N isotope enrichment using NanoSIMS (Fig. 7). After exposure to soil for 60 d, exterior surfaces of PyOM were covered with unlabeled nSOC. This coverage was uneven and showed thicker coatings of unlabeled soil C in some locations than others.

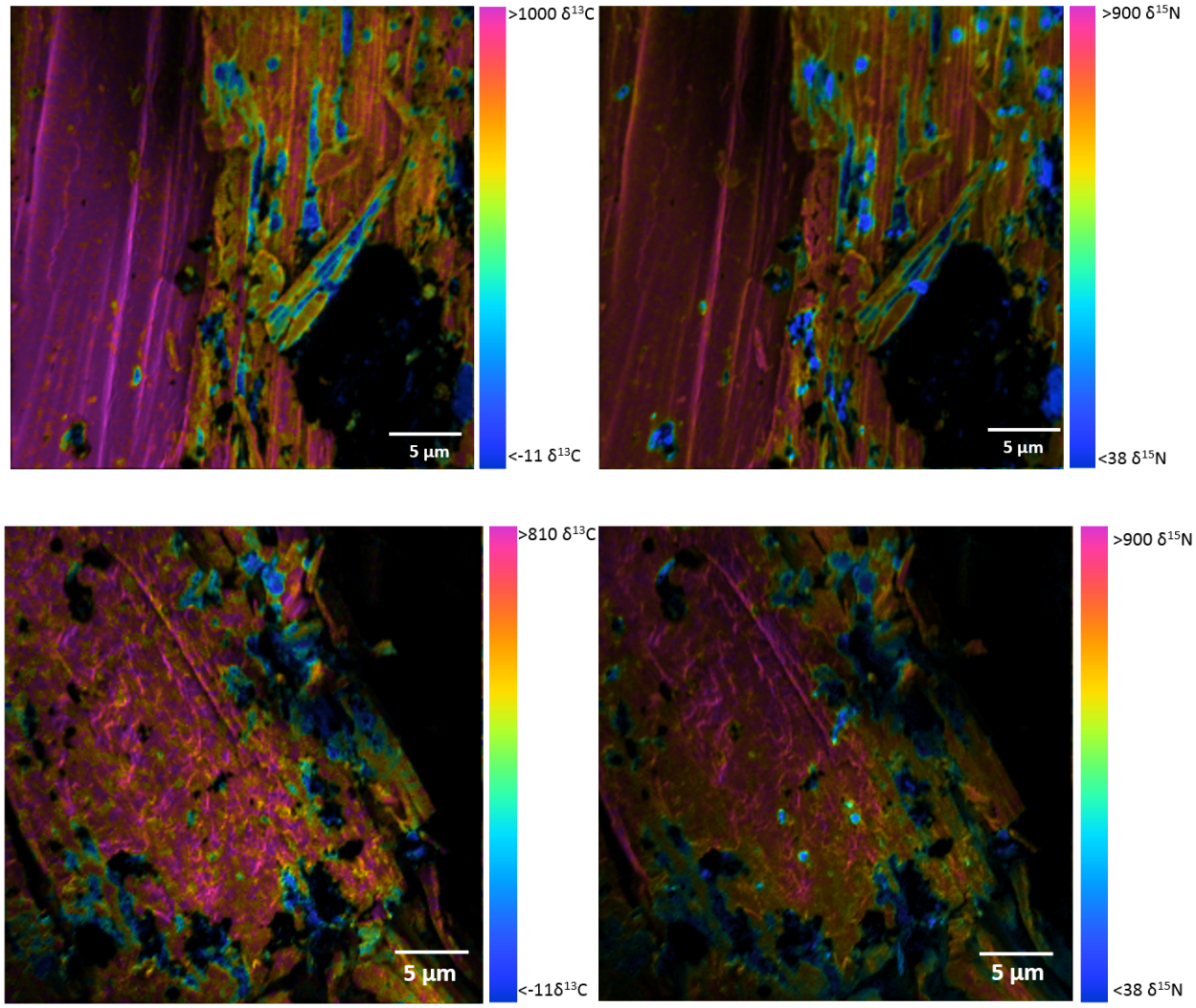

Fig.7. NanoSIMS analyses of isolated PyOM particles with and without exposure to soil; bright pink colors indicate enriched material of the original PyOM and blue colors indicate natural abundance materials from nSOC. Top panel shows 450PyOM after incubation, bottom shows 600PyOM. Left panel shows ^{13}C enrichment, right panel shows ^{15}N enrichment.

1.4.0 Discussion

1.4.1 Positive and negative priming

We observed positive priming as a result of the addition of relatively larger additions of PyOM (larger than 2 mg g^{-1} soil) to mineral soil over monthly or longer time periods, which is also seen in other studies (Cross and Sohi, 2011; Jones et al., 2011; Whitman et al., 2014b). The observed negative priming by PyOM of 1-34% in comparison to unamended soil was in the same order of magnitude as reported in the meta-analysis by Maestrini et al. (2015) for similar incubation times. By performing several different types of incubations and analyses, we determined that dilution and sorption were more important than other negative priming mechanisms in our study.

1.4.2 Dilution mechanism

The observation that daily nSOC mineralization largely converged by day 7 (Fig. 1a) may indicate that short-term processes dominate nSOC mineralization during that period. The reduced nSOC mineralization after additions of inorganic amendments (Fig. 1b,c,d) suggests either dilution or adsorption as the mechanism for negative priming, as no organic substrate was added. The low surface area of the added sand with typically low DOC adsorption (Liang et al., 1996; Kothawala et al., 2000; Clausen et al., 2001) suggests that the resultant reductions in nSOC can be mainly explained by dilution. Extrapolation of decreasing surface area to a hypothetical amendment with no surface area at equivalent volume to the added PyOM indicates a dilution contribution of 1.8 mg CO_2-C g^{-1} C or 20% of the reductions observed with PyOM pyrolyzed at 450°C over the first 7 days. This suggests that dilution is a significant negative priming mechanism, at least initially. However, the greater negative priming with PyOM than explainable

by surface area and the continuously lower daily mineralization of nSOC with PyOM additions beyond the first 7 days indicate that surface interactions may be even more important than dilution which is discussed further below (supplementary online Figure S1).

1.4.3 Substrate switching and co-metabolism

Substrate switching can only account for the amount of PyOM respired to compensate for reductions of nSOC mineralization. Substrate switching may therefore explain up to 100% of the cumulative negative priming observed for PyOM produced at 200°C with a comparatively high concentration of volatiles (Table 1), but not more than 24% for the 300PyOM and on average not more than 13% for the additions of PyOM made at higher temperature (Fig. 2) with comparatively low concentrations of volatiles, for 450PyOM even as low as 1% (Fig. 1). In addition, PyOM produced at the highest tested temperature of 700°C (with negligible volatile concentration) contributed little to microbial biomass (0.07%), had very little mineralizable C, and, especially between day 40-60 mineralized only 0.0076 mg CO_2-C g^{-1} soil d^{-1}, which was far below the continued daily reduction of nSOC mineralization of 0.12 mg CO_2-C g^{-1} soil d^{-1}.

Co-metabolism did not cause a significant net increase in nSOC mineralization with any of the tested PyOM. This, however, is not sufficient evidence to conclude that co-metabolism did not occur but merely indicates that it was less important than the sum of all negative priming mechanisms together. Co-metabolism is seen as a process that may last longer than both dilution and substrate switching, but, similar to substrate switching, may occur concomitant with CO_2 production from the added substrate (Blagodatskaya and Kuzyakov, 2008). Our data indicate that co-metabolism may have occurred early in the incubation (Fig. 3), but could not be detected at or

beyond 40 days, when daily PyOM mineralization decreased to less than 12% of the daily reduction in nSOC mineralization. Desorption of nSOC by additions of DOC contained in PyOM was unlikely to be a relevant mechanism, since PyOM additions account for only 3% or less of existing soil DOC.

1.4.4 Inhibition

Microbial biomass did not decrease with PyOM additions, suggesting that inhibition of the microbial community did not play a role in explaining negative priming. It should be kept in mind that our measurements may have underestimated total microbial biomass with PyOM additions in comparison to no additions, as no adjustments were made for a greater adsorption of any organic matter released from lysed cells during fumigation to the PyOM than the soil, as suggested by the greater DOC adsorption to PyOM than soil (Fig. 6). This likely underestimated the amount of microbial biomass in the presence of PyOM for fresh and aged PyOM (Liang et al., 2010; Dai et al., 2017). Despite this potential methodological issue, if PyOM was indeed adsorbing additional MB-C, the initial MB would have to be higher in PyOM treatments, further supporting a lack of microbial inhibition. One can assume that if the added PyOM was killing microbes (and thus causing negative priming due to a lower population of respiring organisms) the microbial biomass would be less than the unamended control. This mechanism was tested in this study by excluding changes induced as part of varying pH, water or nutrient availability, as these were all adjusted. This result corroborates earlier studies that also did not find inhibition due to organic or non-nutrient inorganic compounds in PyOM (Bruun et al., 2008; Kolb et al., 2009; Maestrini et al., 2014). As mentioned above, microbial biomass quantification in our study was not adjusted for adsorption and likely underestimated the amount of microbial biomass in

the presence of PyOM, which would reinforce the conclusion that the presence of PyOM did not have a toxic effect on the microbial population.

1.4.5 Adsorption

Greater adsorption of DOC to PyOM than to soil can quantitatively explain the lower mineralization of nSOC in the presence of PyOM. Sorption has been proposed as a likely mechanism by several authors (Kuzyakov et al., 2009; Cross and Sohi 2011; Zimmerman et al., 2011; Maestrini et al., 2014; Whitman et al., 2014b) due to PyOM's high surface area, porosity, charge, and overall highly adsorptive characteristics (Ahmad et al., 2013). Our adsorption isotherms showed 19 times greater DOC sorption to the 450PyOM than to the ashed subsoil and an even greater sorption than to the topsoil. Significant removal of DOC of 26-52% by PyOM was also reported in organic horizons (Pietikäinen et al., 2000). The 750PyOM was capable of adsorbing 3 times more DOC than the 450PyOM compared to only about 1.2 times more negative priming than the 450PyOM. The lower reduction in SOC mineralization compared to the increase in DOC adsorption data could be caused by the vast differences in experimental practice. In the adsorption experiment, DOC, soil and PyOM were all freely suspended in water where they can more easily interact, whereas in the incubation, although the soils are moist, there is much less mobility of DOC and nSOC and therefore overall less interaction. However, the comparison illustrates that adsorption is quantitatively a likely process.

Our NanoSIMS data indicated that SOC was indeed present on the surfaces of PyOM. The 450 and 600PyOM both showed natural abundance $\delta^{13}C$ values on the surface of the highly labeled PyOM, indicating the possibility that nSOC was adsorbing to PyOM surfaces. Whether this co-

location of PyOM and nSOC actually led to interactions and how strong these were cannot be discerned by NanoSIMS. The patchiness and apparent accrual of SOC in micro-meter-sized cavities on PyOM surfaces may indicate retention mechanisms beyond uniform adsorption. The accrual of nSOC along discernable morphological features of the PyOM may serve as an indication of explainable mechanisms. Whether such patchiness is a result of the surface morphology (e.g., entrapment of nSOC in large pores) or charge properties as shown on mineral surfaces (Vogel et al., 2014) is not clear.

1.4.6 Comparison of mechanisms

Using the data from this suite of experiments, we suggest that the most likely mechanism of the negative priming observed is sorption, with dilution also being a significant contributor. We further suggest that substrate switching and inhibition mechanisms do not contribute significantly to negative priming interactions. Although we did observe substrate switching, this only accounted for 1.2% of negative priming with dilution making up 20% (Fig. 8). The majority of the remaining negative priming (85%) may be due to adsorption based on our adsorption isotherm assay combined with NanoSIMS data. Unlike substrate switching, adsorption interactions between PyOM and nSOC may be more long-lasting, with net negative priming continuing for a longer period of time (Zimmerman et al., 2011). The duration of this negative priming may be limited by the saturation of adsorption sites, but it is not known if saturation will eventually limit negative priming by adsorption. Because the isotherms indicate a several-fold greater maximum adsorption than emission reductions of SOC after 60 days, one may expect negative priming by adsorption to continue. The negative priming observed 9 years after PyOM addition (Weng et al., 2017) and in PyOM-rich Amazonian Dark Earths that are

several thousand years old (Liang et al., 2010) suggests that adsorption on PyOM surfaces as quantified in our study through batch adsorption experiments may not be sufficient to explain the accrual of nSOC. Whether PyOM effects on signaling between microorganisms (Masiello et al., 2013) or electrochemical processes (Sun et al., 2017) play a role for priming in the presence of PyOM, remains to be quantified. We conclude that positive priming through co-metabolism is also occurring early in the incubation with a 38% increase in nSOC mineralization, though is overwhelmed by negative priming.

The proportions of different mechanisms responsible for negative priming shown here for PyOM pyrolyzed at 450°C (Fig. 8) will vary with PyOM properties as shown here and in other studies (Zimmerman et al., 2011), but also with soil type and SOC properties (Whitman et al., 2014b).

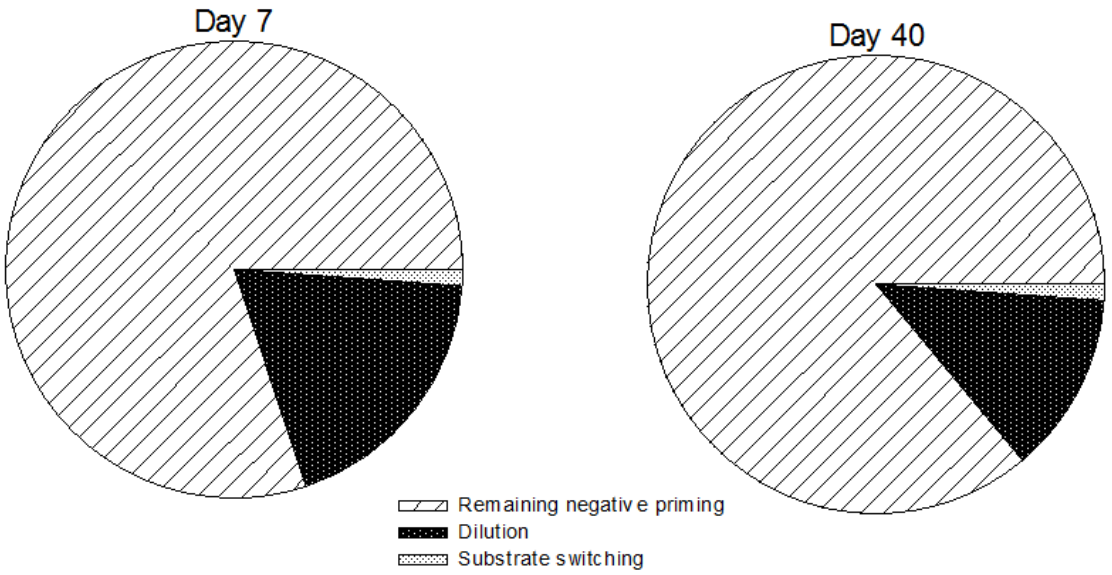

Fig. 8. Proportion of negative and positive priming of nSOC by PyOM (pyrolyzed at 450°C; added at 10 mg g^{-1}) attributed to different mechanisms for day 7 and 40.

1.5.0 Conclusion

Dilution accounted for a significant portion of negative priming, but adsorption is the most likely explanation for the majority of negative priming by addition of PyOM observed in this study when produced at 300°C and above. Substrate switching was able to explain reductions in nSOC mineralization after additions of weakly charred (200PyOM) OM. Sorption of nSOC on PyOM surfaces has the potential for long-term carbon storage as the nSOC is bound to the surface of persistent PyOM and may thereby be protected from mineralization. Given that PyOM naturally exists widely in our soils, and forest fires are likely to increase, these results indicate that priming should, in the future, be incorporated in biochar management and accounted for in carbon cycling models. In order to correctly parameterize such models, more long-term studies and field experiments with and without plants must be conducted to ensure that our results are representative of real-world nSOC interactions. The fate of adsorbed nSOC should be further examined as it is not clear whether adsorption of microbial or plant matter constitutes the bulk of the retained nSOC, and whether eventual desorption or in-situ mineralization may remobilize it, reversing the negative priming observed here.

References

Abatzoglou J, Williams A. (2016) Impact of anthropogenic climate change on wildfire across western US forests. *National Academy of Sciences of the United States of America* Vol 113 no 42: 11770-11775.

Ahmad M, Rajapaksha AU, Lim JE, Zhang M, Bolan N, Mohan D, Vithanage M, Lee SS, Ok YS. (2013). Biochar as a sorbent for contaminant management in soil and water: a review. *Chemosphere* 99: 19-33.

Bell MJ, Worrall F. (2011) Charcoal addition to soils in NE England; a carbon sink with environmental co-benefits? *The Science of the Total Environment.* 409: 1704-1714.

Bingeman CW, Varner JE, Martin WP. (1953) The effect of the addition of organic materials on the decomposition of an organic soil. *Soil Science Society of America Journal* 17: 34–38.

Bird MI, Wynn JG, Saiz G, Wurster CM, and McBeath A. (2015) The pyrogenic carbon cycle. *Annual Review of Earth and Planetary Sciences 43*: 273-298.

Black C, Evals D, White J, Ensminger L, Clark F. (1965) Methods of Soil Analysis Part 1: Physical and Mineralogical Properties, Including Statistics of Measurement and Sampling. American Society of Agronomy, Number 9 in Agronomy Series. Madison, Wisconsin., pp 281.

Blagodatskaya E, Kuzyakov Y. (2008) Mechanisms of real and apparent priming effects and their dependence on soil microbial biomass and community structure: critical review. *Biology and Fertility of Soils* 45(2):115-131

Bruun S, Jensen ES, Jensen LS. (2008) Microbial mineralization and assimilation of black carbon: dependency on degree of thermal alteration. *Organic Chemistry* 39: 839-845.

Bruuslema T, Duxbury J. (1996) Simultaneous measurement of soil microbial nitrogen, carbon, and Carbon Isotope Ratio. *Soil Science Society of America Journal* 60: 1787-1791.

Chen J, Lui X, Zhang B, Lu H, Chi Z, Pan G, Li L, Zheng J, Zhang X, Wang J, Yu X. (2013) Biochar soil amendment increased bacterial but decreased fungal gene abundance with shifts in community structure in a slightly acid rice paddy from Southwest China. *Applied Soil Ecology* 71:33-44.

Cheng CH, Lehmann J, Thies JE, Burton SD. (2008) Stability of black carbon in soils across a climatic gradient. *Journal of Geophysical Research* 113:1–10.

Ciais P, Sabine , Bala G, Bopp L, Brovkin V, Canadell J, Chhabra A, DeFries R, Galloway J, Heimann M, Jones C, Le Quéré C, Myneni RB, Piao S, Thornton P. (2013) Carbon and Other Biogeochemical Cycles. In: Climate Change (2013) The Physical Science Basis. Contribution of Working Group I to the Fifth Assessment Report of the Intergovernmental Panel on Climate Change [Stocker TF, Qin D, Plattner G-K, Tignor M, Allen SK, Boschung J, Nauels A, Xia Y,

Bex V, and Midgley PM (eds.)]. Cambridge University Press, Cambridge, United Kingdom and New York, NY, USA.

Clausen L, Fabricius I, and Madsen L. (2001) Adsorption of pesticides onto quartz, calcite, kaolinite, and α-alumina. *Journal of Environmental Quality* 30:846-857.

Cross A, Sohi SP. (2011) The priming potential of biochar products in relation to labile carbon contents and soil organic matter status. *Soil Biology and Biochemistry* 43: 2127–2134.

Dai Z, Webster TM, Enders A, Hanley K, Xu J, Thies JE, Lehmann J. (2017) DNA extraction efficiency from soil as affected by pyrolysis temperature and extractable organic carbon of high-ash biochar. *Soil Biology and Biochemistry* 115, 129-136.

Ehleringer JR, Bowen GJ, Chesson L, West A, Podlesak DW, Cerling TE. (2008) Hydrogen and oxygen isotope ratios in human hair are related to geography. *PNAS* 105 (8): 2788-2793.

Enders A, Hanley K, Whitman T, Joseph S, Lehmann J. (2012) Characterization of biochars to evaluate recalcitrance and agronomic performance. *Bioresource Technology* 114: 644-653.

Fang Y, Singh B, Singh BP. (2015) Effect of temperature on biochar priming effects and its stability in soils. *Soil Biology and Biochemistry 80*: 136-145.

Graber ER, Singh B, Hanley K, Lehmann J. (2017) Determination of cation exchange capacity in biochar. In: Singh B, Camps-Arbestain M, and Lehmann J. (eds) Biochar: A Guide to Analytical Methods. CRC Press/Taylor and Francis, Boca Raton, pp. 74-84.

Guerena D, Lehmann J, Thies J, Enders A, Karanja N, Neufeldt H. (2015) Partitioning the contributions of biochar properties to enhanced biological nitrogen fixation in common bean (Phaseolus vulgaris). *Biology and Fertility of Soils* 50, No 4: 79-491.

Jenkinson DS, Brookes PC, Powlson DS. (2004) Measuring soil microbial biomass. *Soil Biology and Biochemistry.* 46: 5-7.

Jones DL, Rousk J, Edwards-Jones G, DeLuca TH, Murphy DV. (2012) Biochar-mediated changes in soil quality and plant growth in a three year field trial. *Soil Biology and Biochemistry* 45: 113–124.

Keith A, Singh B, and Dijkstra FA. (2015) Biochar reduces the rhizosphere priming effect on soil organic carbon. *Soil Biology and Biochemistry* 88: 372-379.

Keith A, Singh B, Singh BP. (2011) Interactive priming of biochar and labile organic matter mineralization in a smectite-rich soil. *Environmental Science and Technology* 45: 9611– 9618.

Kettler TA, Doran JW, Gilbert TL. (2001) Simplified method for soil particle-size determination to accompany soil quality analysis. *Soil Science Society of America Journal* 65: 849-852.

Kolb SE, Fermanich KJ, Dornbush ME. (2009) Effect of charcoal quantity on microbial biomass and activity in temperate soils. *Soil Science Society of America Journal* 73:1173.

Kothawala DN, Moore TR, Hendershot WH. (2008) Adsorption of dissolved organic carbon to mineral soils; A comparison of four isotherm approaches. *Geoderma* 148(1):43-50.

Kuzyakov Y. (2010) Priming effects: Interactions between living and dead organic matter. *Soil Biology and Biochemistry* 42: 1363-1371.

Kuzyakov Y, Friedel JK, Stahr K. (2000) Review of mechanisms and quantification of priming effects. *Soil Biology and Biochemistry* 32: 1485-1498.

Kuzyakov Y, Subbotina I, Chen H, Bogomolova I, Xu X. (2009) Black carbon decomposition and incorporation into soil microbial biomass estimated by 14C labeling. *Soil Biology and Biochemistry* 41: 210–219.

Liang B C, Gregorich G, Schnitzer M, Schulten H-R. (1996) Characterization of Water extracts of two manures and their adsorption on soils. *Soil Science Society of America Journal* 60:1758-1763.

Liang B, Lehmann J, Sohi S, Thies J, O'Neill B, Trujillo L, Gaunt J, Solomon D,Grossman J, Neves G, Luizão J. (2010) Black carbon affects the cycling of non-black carbon in soil. *Organic Geochemistry* 41: 206–213.

Laird DA. (2008) The charcoal vision: a win–win–win scenario for simultaneously producing bioenergy, permanently sequestering carbon, while improving soil and water quality. *Agronomy journal 100*(1): 178-181.

Lehmann J, Skjemstad JO, Sohi S, Carter J, Barson M, Falloon P, Coleman K, Woodbury P, Krull E. (2008) Australian climate-carbon cycle feedback reduced by soil black carbon. *Nature Geoscience* 1: 832–835.

Masiello C, Chen Y, Gao X, Lui S, Cheng H, Bennett M, Rudgers J, Wagner D, Zygourakis K, Silberg J. (2013) Biochar and microbial signaling: production conditions determine effects on microbial communication. *Environmental Science and Technology* 47: 11498-11503.

Maestrini B, Herrmann AM, Nannipieri P, Schmidt MWI, Abiven S. (2014) Ryegrass-derived pyrogenic organic matter chances organic carbon and nitrogen mineralization in a temperate forest soil. *Soil Biology and Biochemistry* 69:291-301.

Maestrini B, Nannipieri P, Abiven S. (2015) A meta-analysis on pyrogenic organic matter induced priming. *Global Change Biology Bioenergy* 7: 577-590.

Nelson DW, Sommers LE. (1996) Total carbon, organic carbon and organic patter. *In* Sparks DI. Methods of soil analysis. Part 3, 3rd ed. SSSA. Book ser. 5. SSSA. Madison, WI. pp 961-1010.

Pietikäinen, J., Kiikkila, O. and Fritze, H. (2000) Charcoal as a habitat for microbes and its effect on the microbial community of the underlying humus. *Oikos* 89, 231-242.

Qiao N, Xu X, Hu Y, Blagodatskaya E, Lui Y, Schaefer D, Kuzyakov Y. (2016) Carbon and nitrogen additions induce distinct priming effects along an organic-matter decay continuum. *Scientific Reports* 6, 19865.

Santín C, Doerr SH, Kane ES, Masiello CA, Ohlson M, Rosa JM, Preston CM, Dittmar T. (2016) Towards a global assessment of pyrogenic carbon from vegetation fires. *Global Change Biology 22*(1): 76-91.

Stockmann U, Adams MA, Crawford MA, Field DJ, Henakaarchchi N, Jenkins M, *et al.* (2013) The knowns, known unknowns and unknowns of sequestration of soil organic carbon. *Agriculture Ecosystems and Environment* 164 : 80-99.

Sun T, Levin BDA, Guzman JJL, Enders A, Muller DA, Angenent LT, Lehmann J. (2017) Rapid electron transfer by the carbon matrix in natural pyrogenic carbon. *Nature Communications* 8, 14873.

Vance ED, Brookes PC, Jenkinson DS. (1987) Microbial biomass measurements in forest soils: the use of the chloroform fumigation-incubation method in strongly acid soils. *Soil Biology and Biochemistry* 19: 697-702.

Vogel C, Mueller C W, Höschen C, Buegger F, Heister K, Schulz S, Schloter M, Kögel-Knabner I. (2014) Submicron structures provide preferential spots for carbon and nitrogen sequestration in soils. *Nature Communications* 5: 2947.

Wang J, Xiong Z, Yan X, Kuzyakov Y. (2016) Carbon budget by priming in a biochar-amended soil. *European Journal of Soil Biology* 76: 26-34.

Wardle DA, Nilsson MC, Zackrisson O. (2008) Fire-derived charcoal causes loss of forest Humus. *Science* 320: 629–629.

Weng ZH, Van Zwieten L, Singh BP, Tavakkoli E, Joseph S, Macdonald LM, Rose TJ, Rose MT, Kimber SW, Morris S, Cozzolino D. (2017) Biochar built soil carbon over a decade by stabilizing rhizodeposits. *Nature Climate Change 7*(5): 371-376.

Whitman T, Zimmerman A, Bhupinder PS. (2015) Biochar for environmental Management. Chapter 16: Priming effects in Biochar-amended soils: Implications of biochar soil organic matter interactions for carbon storage. Routledge, London.

Whitman T, Enders A, Lehmann J. (2014a) Pyrogenic carbon additions to soil counteract positive priming of soil carbon mineralization by plants. *Soil Biology and Biochemistry. 73: 33-41*.

Whitman T, Zhu Z, Lehmann J. (2014b) Carbon mineralizability determines interactive effects on mineralization of pyrogenic organic matter and soil organic carbon. *Environmental Science and Technology 48* (23): 13727–13734.

Witt C, Gaunt J, Galicia C, Ottow J, Neue H. (2000) A rapid chloroform-fumigation extraction method for measuring soil microbial biomass carbon and nitrogen in flooded rice soils. *Biology and Fertility of Soils* 30: 510-519.

Zimmerman AR, Gao B, Ahn MY. (2011) Positive and negative carbon mineralization priming effects among a variety of biochar-amended soils. *Soil Biology and Biochemistry 43*(6): 1169-1179.

Supplementary Information

Priming mechanisms associated with pyrogenic organic matter additions to soil

Silene DeCiucies[1], Thea Whitman[2], Dominic Woolf[1], Akio Enders[1], Johannes Lehmann[1,3]*

[1]Soil and Crop Sciences, School of Integrative Plant Science, Cornell University, Ithaca, NY 14850, USA

[2]Department of Soil Science, University of Wisconsin, Madison, WI 53706, USA

[3]Atkinson Center for a Sustainable Future, Cornell University, Ithaca, NY 149850

*Corresponding author, email: CL273@cornell.edu

Table of contents for supporting information

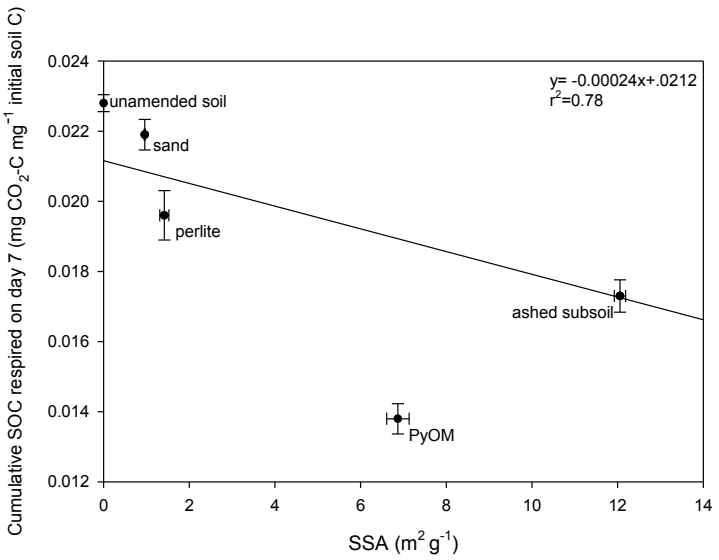

Figure S1. Cumulative nSOC mineralization up to day 7 as related to the specific surface area (SSA) (means and standard errors, n=5; for respiration, n=1or SSA (error calculated from 5-point regression of line of once transformed BET equation); regression includes only sand, perlite and ashed subsoil).

1. Supplementary Discussion

Surface area of PyOM and additional dilution amendments were assayed using both CO_2 and N_2 BET analysis. CO_2 is considered to most accurately measure the nano-porosity of PyOM (Kwon and Pignatello, 2005) and to obtain total surface area that includes very small nanometer-sized pores. We propose that the SSA obtained with N_2 is a more appropriate assessment of the SSA available for DOC adsorption within the scope of this experiment, because the micropores accessed using the CO_2 assay are most likely inaccessible to DOC particles sized up to 0.45µm and therefore larger than the majority of captured by CO_2. Figure S1 uses N_2-SSA data combined with nSOC mineralization after 7 days to determine a regression, whereby the contribution of dilution on nSOC mineralization was quantified by using the y-intercept as a theoretical amendment with no surface area.

References

Kwon S. and Pignatello J.J. (2005) Effect of natural organic substances on the surface and adsorptive properties of environmental black carbon (char): pseudo pore blockage by model lipid components and its implications for N_2-probed surface properties of natural sorbents. Environ. Sci. Technol. **39**, 7932-7939.

Table S1. Properties of amendments and proportion of SOC respired on day 7 (means, n=5).

Amendment	Bulk density ($g\ cm^{-3}$)	Mass added (g)	SSA N_2 ($m^2 g^{-1}$)	SSA CO_2 ($m^2\ g^{-1}$)	Proportion SOC respired, Day 7 (mg CO_2-C mg^{-1}initial SOC)
450°C PyOM	0.175	0.238	6.8705	192.61	0.0138
Ashed temperate subsoil	1.15	1.564	12.054	11.46	0.0173
Perlite	0.15	0.204	1.4173	-0.177	0.0196
Quartz sand	4.59	6.24	0.963	-0.19	0.0219
Control treatment	n/a	0.0	n/a	n/a	0.0228

n/a not applicable

Table S2. Microbial biomass and microbial quotient (n=4).

Treatment	Microbial biomass (mg MB-C g^{-1} soil)	Microbial biomass from amendment (mg MB-C g^{-1} soil)	Total CO_2 respired (mg CO_2-C g^{-1} soil)	Metabolic quotient (mg CO_2-C mg^{-1} MB-C day^{-1})
Topsoil, unamended	0.86	n/a	0.0028	0.0032
Topsoil, 750 PyOM	1.28	0.0009	0.0024	0.0018
Topsoil, 450 PyOM	1.07	0.0008	0.0026	0.0024
Topsoil, 300 PyOM	1.25	0.004	0.0025	0.0020

n/a not applicable

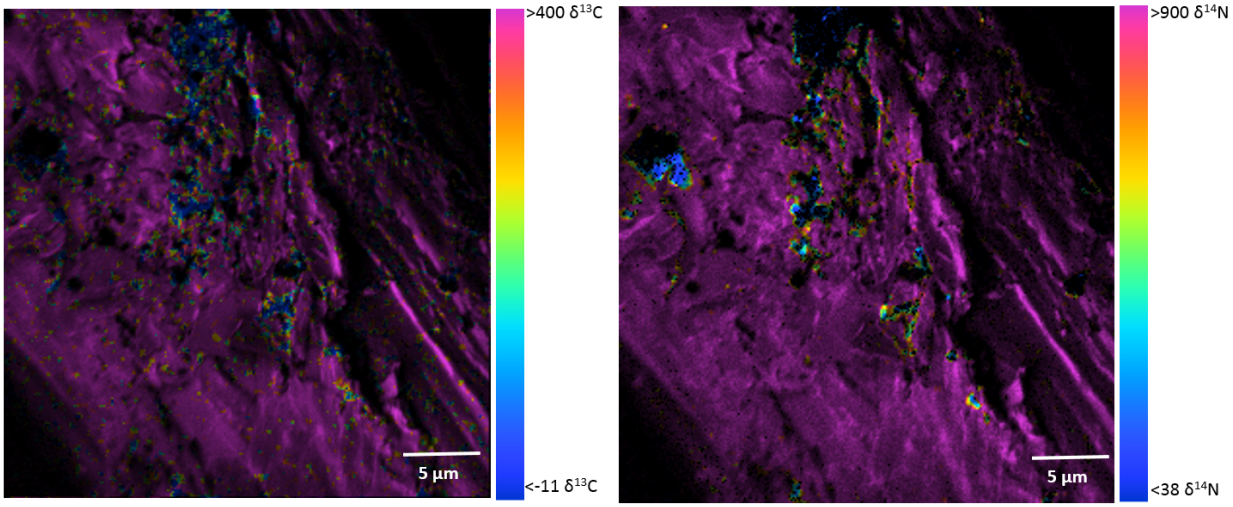

Figure S2. NanoSIMS image of labeled 450 PyOM not incubated with soil.

CHAPTER 2

Priming of organic carbon in different soil horizons after additions of charred and uncharred organic matter

Silene DeCiucies[1], Thea Whitman[2], Dominic Woolf[1], Akio Enders[1], Johannes Lehmann[1,3]*

[1]Soil and Crop Sciences, School of Integrative Plant Science, Cornell University, Ithaca, NY 14850, USA

[2]Department of Soil Science, University of Wisconsin, Madison, WI, 53706, USA
[3]Atkinson Center for a Sustainable Future, Cornell University, Ithaca, NY, 14850

*Corresponding author, email CL273@cornell.edu

Keywords: Priming, stable isotopes, biochar, soil carbon

Abstract

This study investigates short-term priming of native soil organic carbon (nSOC) by pyrogenic organic matter (PyOM) and uncharred biomass additions in organic soil horizons dominated by plant residues in comparison to mineral horizons dominated by microbial residues. CO_2 respired over 50-90 days was partitioned between nSOC and ^{13}C-enriched PyOM or biomass using a stable isotope analyzer. Additions of uncharred biomass induced 24% and 30% greater cumulative nSOC mineralization over 60 days in temperate top- and subsoils with C contents of 5% and 1%, respectively. In contrast, PyOM additions caused 24% ($p < 0.01$) and 6.67% ($p = 0.12$) lower mineralization in the same soil horizons over 60 days. Whereas the reduction of nSOC mineralization was in a similar order of magnitude as the PyOM mineralization in the subsoil, PyOM mineralization in the topsoil accounted for only 3% of the reduction in nSOC mineralization indicating that a mechanism in addition to substrate switching was responsible for the amount of negative priming observed in the topsoil. In the boreal and temperate organic horizons PyOM additions had no significant effects on nSOC mineralization, regardless of presence of soil minerals. Increasing the biomass addition to the boreal O horizon from 0.01 to 50% w/w increased nSOC mineralization by 25% with a 17-fold increase in the fraction of microbial biomass C from the added biomass. Similar increases in PyOM addition did neither increase nSOC mineralization nor the fraction of microbial biomass derived from PyOM. Negative priming by PyOM additions mainly depended on the form of nSOC and was only observed in mineral horizons dominated by nSOC of microbial origin with low C/N ratios. Increased carbon storage through negative priming with PyOM may only prove significant in select soil profiles and ecosystems.

2.1 Introduction

Pyrogenic organic matter (PyOM) is an important soil carbon (C) pool and is estimated to make up on average 14% of global soil organic C (SOC) (Reisser et al., 2016). PyOM is produced in terrestrial systems naturally through vegetation fires (Czimczik and Masiello, 2007), and is tied to human activity from the earliest cookfires and burn pits (Eckmeier et al., 2010) to purposeful fire management (Downie et al., 2011). Soil PyOM is not currently included in C cycling models despite the fact that in the past several years the potential impacts of PyOM on native soil organic carbon (nSOC) mineralization have been demonstrated (Laird, 2008; Maestrini et al., 2015; Whitman et al., 2015; Wang et al., 2016). Such priming of nSOC by additions of uncharred OM has been described for some time (Bingeman et al., 1953; Kuzyakov 2000, 2010), but studies on the role of PyOM in priming have only been conducted over the past decade (Wang et al., 2016). Priming can be positive in that the mineralization rate increases with addition, or negative, in that the rate of mineralization decreases (Bingeman et al., 1953).

Priming studies in recent literature (Wang et al., 2016) have resulted in lower and higher nSOC mineralization after PyOM addition. Reasons for the variable effects are the many mechanisms by which PyOM may elicit greater or lower nSOC mineralization (Whitman et al., 2015), varying PyOM (Zimmerman et al., 2011; Fang et al., 2015) and soil properties (Luo et al., 2011). Since several mechanisms may operate at the same time, potentially the most important difference is the soil type itself. However, few systematic studies have been conducted that probe the effects individual soil properties may have.

Past studies have indicated that the nSOC amounts as a result of cropping may affect the direction and magnitude of priming (Cross and Sohi, 2011). Specifically, the amount of easily mineralizable nSOC is an important factor in the effect of PyOM additions on nSOC (Cross and

Sohi, 2011; Keith et al., 2011; Whitman et al., 2014b). Adding plant litter (Keith et al., 2011) enhanced negative priming by PyOM additions, suggesting that mineralization of plant-derived nSOC with high C/N ratios is reduced to a greater extent by PyOM than total nSOC. One of the largest increases in nSOC mineralization was inferred from C losses of boreal organic (O) horizons using litterbags without any mineral soil (Wardle et al., 2008). Litter layers and O horizons do not only differ in their mineralizability from mineral horizons, but also in their composition from underlying mineral soil (Kögel-Knabner et al., 1988; Rumpel et al., 2004). Consolidating these results by direct comparison of soil horizons with varying mineral and nSOC contents has not been done.

Our objective was to determine if the amount or form of nSOC has a greater effect on priming by charred and uncharred OM. We hypothesized that soils with more nSOC would have a greater potential for negative priming by PyOM and for positive priming by uncharred OM, because more nSOC would be available to interact with the amendments. Soils and soil horizons with a greater proportion of plant-derived nSOC and consequently higher C/N ratios are more easily primed than those with a greater proportion of microbially processed nSOC and therefore lower C/N ratios. Note that for the remainder of this paper we use C/N ratio as a convenient proxy for extent of microbial processing.

2.2 Materials and Methods

2.2.1 Biomass production

Preble shrub willow (*Salix viminalis x S. miyabeana*) was grown in a Percival AR 100L3 CO_2 growth chamber (Percival, Perry, IA, USA) with a $^{13}CO_2$-enriched atmosphere to produce enriched biomass.

159 The plants were subjected to an 18-h photoperiod at 24°C, and 6 h of darkness at 17°C. A de-
160 humidifier was used to control humidity and during the photoperiod CO_2 levels were kept at 400
161 ppm. $^{13}CO_2$ was provided to the plants once first buds emerged from the willow cuttings. Over
162 the course of their 6-month growth period, 20 L of 99% ^{13}C-CO_2 was supplied at an increasing
163 rate. The gas was delivered using a plastic CO_2 impermeable bag attached to 1mm nylon tubing
164 which delivered gas through a solenoid peristaltic pump into the growth chamber. This set-up
165 allowed for a slow steady stream of CO_2 during the photoperiod. Concurrently, natural
166 abundance willow was grown in ambient CO_2 greenhouse conditions to provide a near-identical
167 product that could be used to dilute the labeled material to be used for some experiments.
168 Both sets of willows were grown in Cornell potting mix from 0.3 m willow cuttings
169 obtained from Cornell's Willow Research Farm in Geneva, NY and were watered and fertilized
170 on the same schedule. Willow was harvested 3 times throughout the 6-month growing period.
171 At each harvest, all of the new growth was removed from the stem with the exception of 2-3
172 nodes which were left for re-growth. The willow was harvested before reproductive maturity at
173 each harvest. The plant material was separated into stems and leaves and oven-dried at 70°C.
174
175 2.2.2 PyOM production
176 Oven-dried willow stems were milled to <2 mm and pyrolyzed in a modified muffle
177 furnace under Argon (Ar). Ramp rate of 2.5°C min^{-1} and 30 min dwell time at 450°C was
178 followed by a slow cool under Ar. To prepare PyOM and uncharred biomass for incubations,
179 they were first shaken in DI water overnight and rinsed to remove easily soluble ash and water
180 soluble material. All PyOM and biomass were pH adjusted to the pH of the soil used in the
181 incubation using 1 M HCl over the course of five days. After pH adjustment, the amendments
182 were rinsed with deionized (DI) H_2O, oven dried at 70°C and sieved to 150-850 µm. The

amendments were assessed for fixed carbon, ash, and volatiles using the Enders et al. (2012) method. Water soluble DOC was quantified by water extraction with a 1:10 (w/v) ratio, shaken for one hour, filtered, and analyzed on a DOC analyzer (Shimadzu TOC-5000A, Columbia, MD, USA). Total C, hydrogen (H), nitrogen (N) and oxygen (O), bulk $\delta^{13}C$ and $\delta^{15}N$ were measured using a Delta V Isotope Ratio Mass Spectrometer (Thermo Scientific, Germany) coupled to a dry combustion analyzer (Carlo Erba NC2500 Elemental Analyzer, Italy). Nitrate (NO_3^-) and ammonium (NH_4^+) were extracted with 2M Potassium Chloride (KCl) and quantified using a continuous flow analyzer (Bran and Luebbe Autoanalyzer, SPX,Charlotte, NC, USA). PyOM was digested in hydrogen peroxide (H_2O_2) and analyzed using Inductively Coupled Plasma Optical Emission Spectrometry (ICP-OES) for elements, CEC was determined using Graber et al. (2017) and pH was determined in DI water using a glass electrode (detection limit of 0.01 pH units) with a PyOM:water ratio of 1:10 (w/v) (Orion 3-Star pH Benchtop; Thermo Electron Corporation, Beverly, MA, USA).

199 Table 1. Properties of PyOM and uncharred biomass from willow stems as they were applied to soil
200 (except pH, which is shown before pH adjustment to the pH of the respective soil as shown in Table 2)

Property (units)	450°C PyOM	Uncharred Biomass
Ash (%)	1.88	0.63
Volatiles (%)	23.9	92.5
Fixed carbon (%)	74.3	6.9
pH (H_2O) before adjustments	10.77	5.38
Extractable NO_3^- and NO_2^- (mg NO_3+NO_2-N kg^{-1})	1.06	11.6
Extractable NH_4^+(mg NH_4-N kg^{-1})	15.1	106.8
DOC (mg C kg^{-1})	275.4	5776.0
DOC (g C kg^{-1} C)	0.36	10.31
Total H (%)	3.2	6.9
Total O (%)	12.8	47.8
Total C (%)	76.5	56.0
Inorganic C (%)	0	0
Total N (%)	3.05	1.77
$H/C_{organic}$ (mol mol^{-1})	0.49	1.46
$O/C_{organic}$ (mol mol^{-1})	0.12	0.64
C/N (g g^{-1})	25.1	31.6
Total P (mg kg^{-1})	1965.1	338.2
Total K (mg kg^{-1})	2291.7	1844.6
Total Ca (mg kg^{-1})	4433.3	2219.3
Total Mg (mg kg^{-1})	911.2	265.3
Total Na (mg kg^{-1})	134.3	95.1
Bulk ^{15}N (atom %)	7.71	8.19
Bulk $\delta^{13}C$ (‰)	693.6	748.1

201

202 2.2.3 Soils

203

204 Soils in this investigation were chosen based on having a range of nSOC contents and

205 forms while maintaining the same parent material to control for as many variables as possible.

206 Soil was collected from a mixed deciduous forest on Mt. Pleasant in Dryden, NY, USA. The

primary soil used is a Mardin channery silt loam- a coarse loamy, mixed, active, mesic typic Fragiudept that had no instance of burning in recorded history. The entire O horizon (Oi and Oe) was collected (0.0-0.02 m) as well as the A (0.02-0.2 m) and B (BE and Bw) horizons (0.2-0.4 m). These will be referred to here as temperate O-horizon, temperate topsoil, and temperate subsoil, respectively. From these soils, an artificial soil was created by mixing ashed temperate subsoil (ashed at 500°C for 8 h in a muffle furnace) and the temperate O-horizon to achieve the same nSOC content as the temperate topsoil (Table 2). This soil will further be referred to as the temperate-O + ashed subsoil. In addition, the top 0.01 m of an O-horizon was obtained from a boreal forest soil in northern Sweden (GPS coordinates 65.38303, 19.43586; Wardle et al., 2008) and referred to as boreal-O. All soils were homogenized, sieved (<2 mm), and air dried in preparation for the incubation.

Field capacity of each soil and each soil mixture of soil+amendment was determined using the modified method from Black et al. (1965) in PVC tubes having the exact diameter of qorpax jars used in the incubation experiments. Particle size fractionation was done using Kettler et al. (2001). Total C, H, N and O, bulk $\delta^{13}C$ and $\delta^{15}N$, pH, extractable NO_3^- and NH_4^+, and total nutrient contents were measured as described above for PyOM materials. Water extractable C (DOC) was extracted using in DI H_2O using a 1:10 ratio (w v^{-1}), and inorganic C was assessed using the Bernard calcimeter CO_2 displacement method (Nelson, 1996).

228 Table 2. Properties of the investigated soils

Property (units)	Temperate Subsoil	Temperate Topsoil	Temperate-O + ashed subsoil	Temperate-O	Boreal-O
Sand (%)	26.4	15.9	25.9	NA	NA
Silt (%)	57.5	59.5	57.9	NA	NA
Clay (%)	16.1	24.6	16.2	NA	NA
Texture	Silt loam	Silt loam	Silt loam	Organic	Organic
Field capacity (mL g^{-1} soil)	0.43	0.82	1.27	4.02	6.09
Extractable NO_3^- and NO_2^- (mg kg^{-1})	1.34	3.99	1.13	1.45	0.64
Extractable NH_4^+-N (mg kg^{-1})	40.2	45.7	45.9	12.8	24.2
Total C (%)	1.22	5.28	5.62	43.30	46.20
Total N (%)	0.12	0.38	0.21	1.34	1.04
Total P (mg kg^{-1})	195	15	273	383	174
Bulk $\delta^{13}C$ (‰)	-26.1	-27.4	-28.8	-27.2	-29.1
C/N (g g^{-1})	10.2	13.8	26.8	32.3	44.4
Water-extractable DOC (mg C kg^{-1})	127	703	384[a]	2965	3742
Water-extractable DOC (g C kg^{-1} nSOC)	10.4	13.3	6.1	6.9	8.1
Microbial biomass[b] (mg C g $soil^{-1}$)	0.03	0.31	0.22	0.45	4.87
Microbial biomass[b] (mg C g^{-1} nSOC)	2.46	5.81	3.91	0.97	11.23
pH (H_2O)	6.2	4.89	6.00	5.85	3.52

229 [a] Calculated value based on ashed subsoil and temperate-O data.

230 [b] Microbial biomass of unamended soil at the end of the incubation (day 45-90)

231

232 2.2.4 Incubation experiment

233 Incubations took place in 1-L mason jars, whereby 30 mL DI water was poured in the bottom of
234 each jar to maintain 100% humidity. Each jar contained a smaller 60-mL qorpax bottle
235 containing the soil and amendment mixture. Dry soil and dry amendments were added to the jars,
236 mixed, and wetted to achieve 65% field capacity for the soil+amendment mixture. A final wet
237 soil mass of 5.0 g for the boreal and temperate O-horizon, 40 g for temperate topsoil, temperate
238 subsoil, and temperate-O + ashed subsoil were used. One mL of a modified Hoagland's solution

was added to each jar to supply sufficient nutrients to exclude any effects by nutrients contained in amendments (Whitman et al., 2014a). A control treatment with no amendment was included for each soil. PyOM was added to soil at a rate of 10 mg g^{-1} dry soil. Uncharred willow biomass was added based on the equivalent mass used to make PyOM at a 33% conversion rate. Each treatment was replicated four times. The boreal-O, temperate-O, temperate topsoil, temperate-O + ashed subsoil, and temperate subsoil incubations were conducted for 90, 50, 50, 60 and 60 d, respectively. Each incubation was continuously monitored using a Picarro CO_2 stable isotope analyzer (G2201-I, Santa Clara, CA, USA) fitted with a custom-built manifold capable of sampling 112 Mason jars continuously for the entire incubation period. Each sample jar was sampled for 6 min during each sampling period, and subsequently purged with CO_2-free air to re-start at zero CO_2 each period. Data were collected at a rate of 2 measurements per second over the 6-min sampling period, and throughout the 6-min sample purge.

The boreal-O horizon soil was used in a second experiment to determine the effects of different concentrations of PyOM and uncharred biomass on nSOC mineralization. Incubations took place using the same set-up as the soil-C content incubation described above. One g of dry soil was added to each jar, and the amendment was added in concentrations of 0.01, 0.1, 0.5, 1.0, 2.5, 5.0, 10, 30, and 50% by mass. The amendment and soil were mixed and brought to 65% field capacity, bringing each jar to approximately 5.0 grams of wet soil including the amendment. The incubation took place over 30 days.

2.2.5 Microbial biomass

Upon conclusion of the incubation, samples were immediately assayed for microbial biomass (MB) using a modified simultaneous $CHCl_3$ extraction method from Witt et al. (2000). Using a modified method from Bruuslema et al. (1996), the 0.05M potassium sulfate (K_2SO_4) extracts

were oven dried at 50°C in tin capsules and analyzed for total C and $\delta^{13}C$ concentration using a Delta V Isotope Ratio Mass Spectrometer (Thermo Scientific, Germany) coupled to a Carlo Erba NC2500 Elemental Analyzer (Italy). An extraction coefficient of 0.45 was used to determine the total MB (Vance et al., 1987; Jenkinson et al., 2004) and 2-part partitioning was used to attribute microbial biomass-C (MB-C) to either nSOC or amendment-derived C as described below. After MB-C analysis, soils were air-dried and sealed in air-tight storage bottles for later analyses.

2.2.7 Data analyses

Respiration and microbial biomass data were analyzed using R version 3.3.1 (R Foundation for Statistical Computing, Vienna, Austria). Respired CO_2 or microbial biomass C were parsed into nSOC-derived or amendment C (PyOM or uncharred OM) using the following equation:

$$\delta_{measured} = \delta_{nSOC} * (f_{nSOC}) + \delta_{PyOM,OM} * (1\text{-}f_{nSOC})$$

$$f_{nSOC} = \delta_{measured} - \delta_{PyOM.OM} / \delta_{nSOC} - \delta_{PyOM,OM}$$

$$f_{nSOC} * CO_2\text{-C respired} = \text{respired nSOC}$$

Bulk isotopic contents of the amendments ($\delta_{PyOM,OM}$) were used as an endmembers in isotope partitioning equations because bulk PyOM values have been shown to be an appropriate proxy for $^{13}CO_2$ respiration over time (Whitman et al., 2014b). Soil isotope values used in isotope partitioning equations (δ_{nSOC}) were obtained daily by taking the mean $\delta^{13}C$ value for the control. Treatment differences were determined using ANOVA analysis and Tukey corrections for multiple comparisons as well as two-sample t-tests between treatments. Cumulative respiration data were analyzed using pairwise comparisons between treatments based on a mixed effects linear model with a random effect added on the sample jar to correct for multiple samplings.

2.3 Results

2.3.1 Mineralization

The boreal-O showed increasing nSOC mineralization 30-40 d after addition of uncharred biomass, but no significant priming after 40 d for the remainder for the incubation. Temperate-O and temperate-O + ashed subsoil (Fig. 1a-c) did not exhibit significant priming with either PyOM or uncharred biomass additions over the period of 60 d examined here. Uncharred biomass additions to the temperate topsoil (Fig. 1d) increased nSOC mineralization after 20 d, whereas additions of PyOM caused significant negative priming after 30 d. By day 50, additions of uncharred biomass resulted in 17% greater, and of PyOM a 24% lower, nSOC mineralization.

Additions of PyOM to temperate subsoil (Fig. 1e) resulted in negative priming by the end of the incubation (7% decrease in nSOC after 60 d, $p = 0.12$). Additions of uncharred biomass resulted in 30% greater cumulative nSOC mineralization by day 10, increasing to 36% by day 50.

In all soils, the cumulative PyOM respiration at day 50 was very low with 0.01-0.24 mg CO_2-C g^{-1} soil (0.14-0.57% of PyOM-C). Uncharred biomass respiration was roughly 100 times higher than PyOM respiration in the topsoil (3.24 mg CO_2-C g^{-1} soil, 23% of biomass-C) and subsoil (4.63 mg CO_2-C g^{-1} soil, 33% of biomass-C). Cumulative mineralization (50 d) of added uncharred biomass exceeded the change in nSOC mineralization for the mineral horizons 4-28 times as a proportion of soil mass, was 10 times lower for the boreal-O horizon and was 70% lower for the temperate-O horizon. In contrast, cumulative mineralization of added PyOM was much lower, and was only 1.3 times greater for the temperate subsoil, and for the remainder of the soils, negative priming of nSOC was even 4-1000 times greater than PyOM respired.

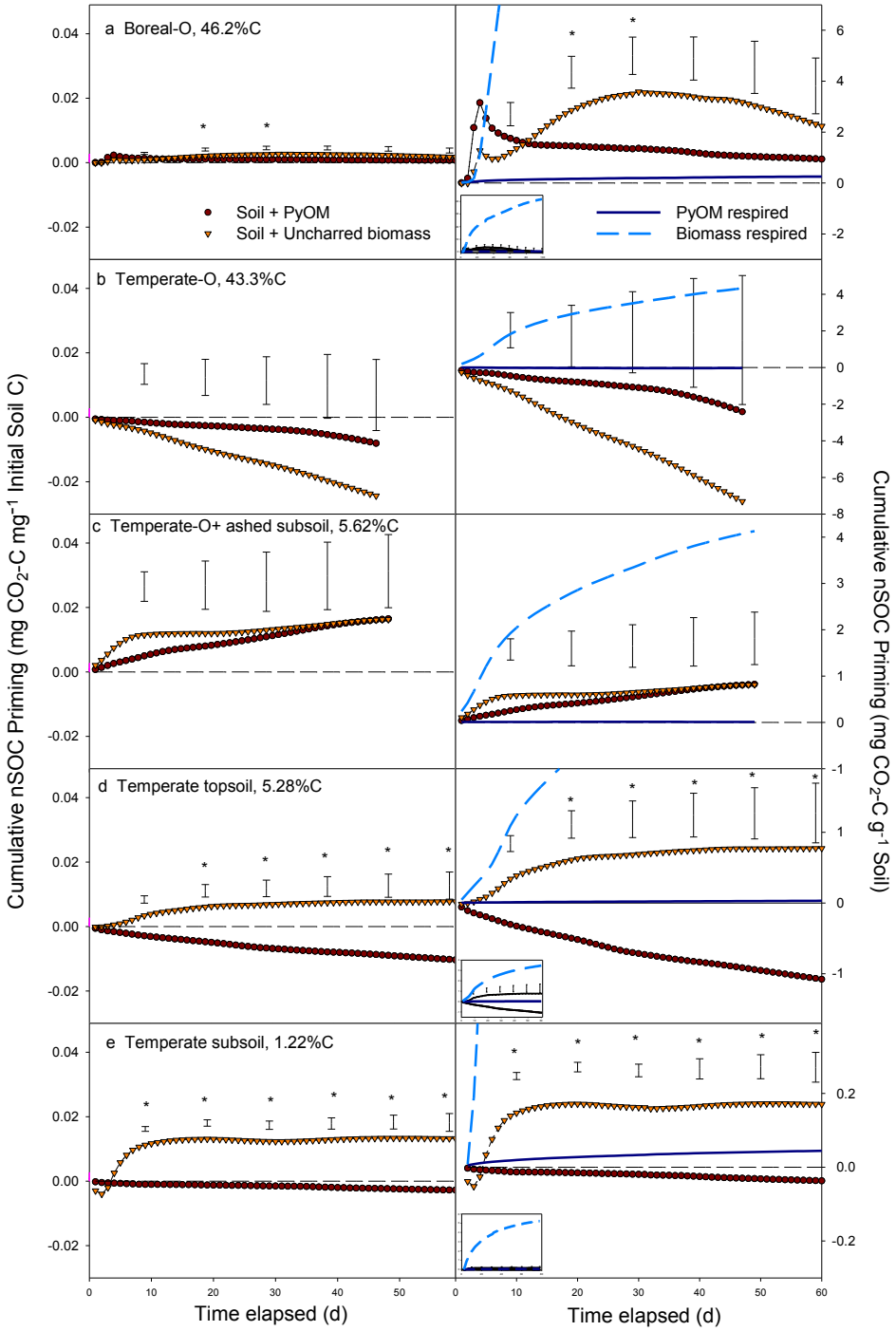

306
307 **Fig. 1.** Cumulative priming of nSOC in comparison to mineralization of amendments after addition of 10
308 mg g^{-1} charred (PyOM) and 30 mg g^{-1} uncharred OM (Biomass). Left panes show mean cumulative nSOC
309 priming per unit initial soil C per day, determined by subtracting CO_2 evolution from unamended control
310 from that of amended soils; dashed black line indicates unamended control; data above this line indicate
311 positive priming, below indicate negative priming. Right panes show mean cumulative nSOC priming
312 per unit soil mass per day; bold dashed (Biomass) and bold solid (PyOM) lines indicate cumulative
313 respiration of the amendment per unit soil mass. (n=4; bars show LSD at $p<0.05$, comparisons only for
314 nSOC).

While increasing biomass additions from 0 to 50% (w/w) resulted in 34% more nSOC respired at day 10 (and 34% at day 50), adding PyOM decreased cumulative nSOC mineralization by 7% on day 10 (and 18% at day 50) (Fig. 2).

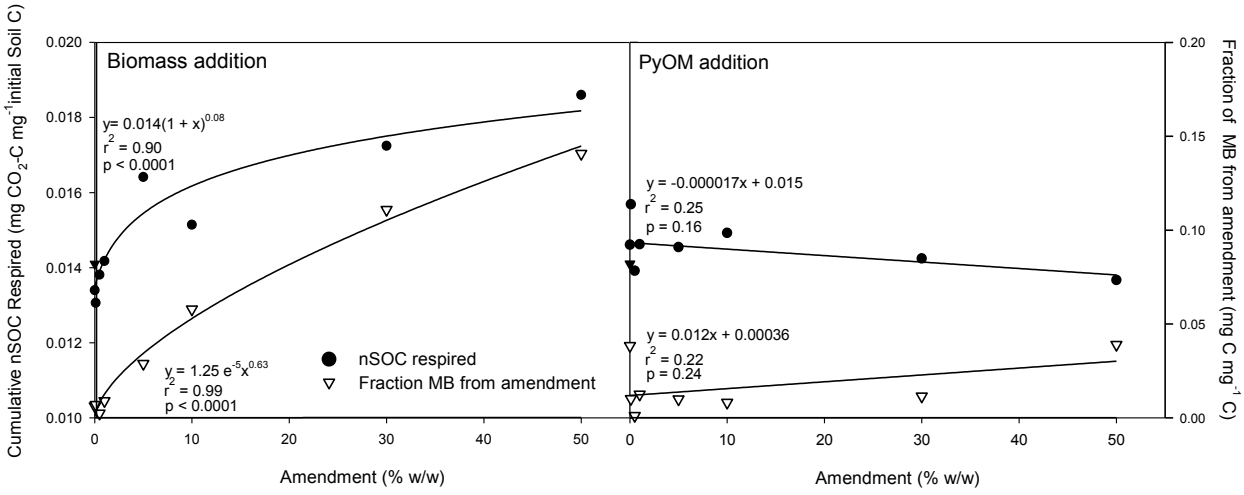

Fig. 2. Cumulative nSOC respired at day 10 and the fraction of microbial biomass (MB) 50 days after adding increasing amounts of uncharred biomass (left) or PyOM (right). Solid black lines indicate regressions for that dataset.

2.3.2 Microbial biomass

Microbial biomass C (MB-C) was 0.45-4.8 mg C g^{-1} soil in the two O horizons, 0.3 mg C g^{-1} soil in the temperate topsoil, and 0.03-0.22 mg C g^{-1} soil in the subsoil and temperature-O + ashed subsoil, and increased with the addition of PyOM in the boreal-O, but did not increase for the other soils (Fig. 3). The proportion of MB-C in nSOC did not change significantly and ranged from 0.97 – 14.5 mg MB-C g^{-1} nSOC (Supplementary Table S2). Except for the temperate-O horizon, the fraction of MB-C derived from the added uncharred biomass was 13-18 times greater than the fraction derived from PyOM for the topsoil and all O horizons. In the subsoil,

however, the fraction of MB-C derived from added uncharred biomass or PyOM was about 3 times greater than in all the other soils.

In the boreal-O soil, with increasing uncharred biomass additions, the fraction of MB-C derived from the amendment increased 17-fold to 0.14, whereas the corresponding fraction from added PyOM did not increase (Fig. 2).

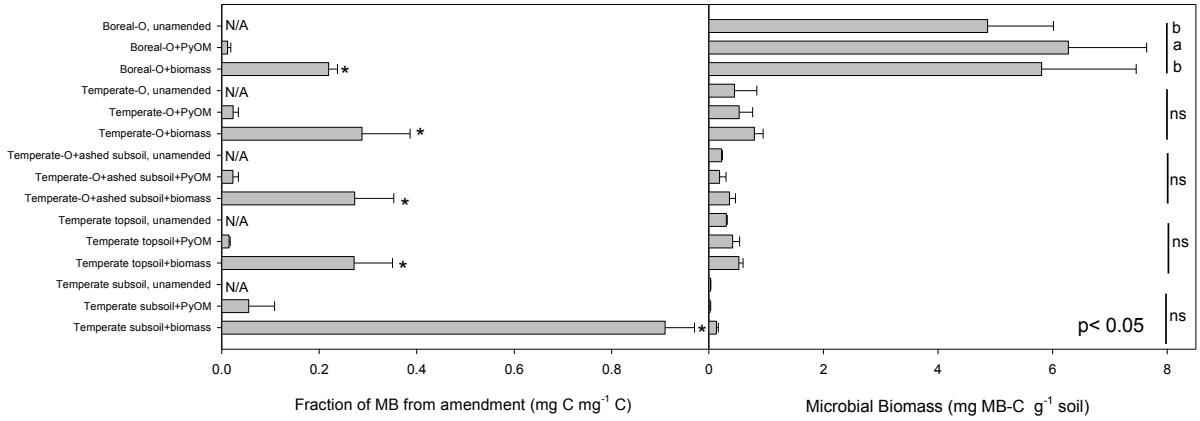

Fig. 3. Microbial biomass (right) and fraction of microbial biomass C from amendment (left) at 90, 50, 50, 60 and 60 days for boreal-O, temperate-O, temperate topsoil, temperate-O + ashed subsoil, and temperate subsoil, respectively. Asterisks indicate where the fraction from PyOM and biomass additions are different within a given soil ($p < 0.05$, means and standard errors, n=4; N/A not applicable as no amendment was added).

2.4 Discussion

2.4.1 nSOC priming after addition of uncharred biomass

The consistently positive priming with uncharred biomass addition can be explained with co-metabolism (Blagodatskaya and Kuzyakov, 2008; Kuzyakov, 2010), whereby the added organic matter is providing the energy to the microbial population to metabolize a greater proportion of nSOC. The lack of increase or decrease in microbial biomass together with a higher proportion of the amendment in microbial biomass supports the notion that actual priming through co-metabolism as a mechanism occurred rather than apparent priming whereby the added amendment would simply increase microbial C turnover, but not nSOC mineralization (Blagodatskaya and Kuzyakov, 2008). The decline in the proportion of positive priming with greater nSOC contents corroborates that C limitation enhanced the positive priming effect by alleviating energy constraints by the microbial community. However, this positive priming by uncharred biomass is largely a question of the added amounts in relation to the amount of nSOC present, since an increasing nSOC mineralization was observed with greater additions of uncharred biomass (Fig. 2).

The forms of nSOC present appear to have had only a minor influence on the magnitude and direction of priming with uncharred biomass. One may speculate whether the higher C/N ratios (used here as a proxy for extent of microbial processing) of the O horizons (temperate-O: 32.3 and boreal-O: 44.4) in comparison to the mineral soils (10.2 and 13.8) may explain why the uncharred biomass addition (31.6) stimulated nSOC mineralization in the mineral rather than organic horizons.

371 2.4.2 nSOC priming after additions of PyOM

372 The lower negative priming observed in low-C subsoil than in higher-C topsoil may be
373 explained by lower DOC in the subsoil (127 g C kg^{-1} soil) than the topsoil (703 g C kg^{-1} soil) that
374 was available to interact with PyOM. This finding is contrary to Whitman et al. (2014b) wherein
375 the depletion of easily mineralizable nSOC by a 6-month pre-incubation of the same soil
376 increased negative priming by PyOM produced at 450°C, albeit with lower nSOC contents of
377 1.07-1.16% than in this study with 1.22-5.28% (Table 2). This difference in nSOC levels
378 resulted in large differences in nSOC mineralization; 250 mg C kg^{-1} soil and 470 mg C kg^{-1} soil
379 for low and high C soils respectively in Whitman et al. (2014b), versus 640 mg C kg^{-1} soil and
380 5380 mg C kg^{-1} soil in sub- and topsoil in this investigation, wherein our subsoil was closer in
381 nSOC content and mineralization to the soil with higher mineralization in Whitman et al.
382 (2014b).

383 The explanation that more available C induces more negative priming, however, does not
384 hold for the O-horizons used in this investigation. These soils exhibited no significant negative
385 priming with PyOM additions but had much greater nSOC and DOC concentrations. At least for
386 the boreal-O horizon, the lack of effects of PyOM on nSOC mineralization was clearly not a
387 result of different ratios of PyOM and nSOC: irrespective of application rate, PyOM did not
388 reduce nSOC mineralization. Therefore, it is more plausible that the form of nSOC determined
389 the direction and magnitude of priming rather than the amount as discussed in more detail below.

390 Several studies (Kuzyakov et al., 2009; Cross and Sohi, 2011; Zimmerman et al., 2011;
391 Maestrini et al., 2014; Whitman et al., 2014b) have suggested that negative priming by PyOM is
392 most likely a result of the sorption mechanism whereby DOC from the soil is adsorbed onto the
393 surface of the PyOM thereby being protected from microbes. This is consistent with our findings.

Unlike applications of uncharred biomass, PyOM was not incorporated to a great extent in microbial biomass and PyOM mineralization was only 3% of the reduction in nSOC mineralization. Therefore, substrate switching is not a likely mechanism explaining the net negative priming by PyOM.

2.4.3 Effect of C-mineral association and nSOC forms on priming interactions

Two factors may be able to explain the differences in nSOC priming effects between different soil horizons observed in this study: nSOC interaction with parent material minerals, and the form of nSOC itself. In order to examine the concept, we compared priming across the studied soils having mostly mineral associated C in the subsoil to O-horizons with no minerals, and from pure litter with high C/N ratios to mainly decomposed OM with low C/N ratios (Fig. 4). Presence of minerals was not sufficient to result in reduced nSOC mineralization after additions of PyOM. Despite the fact that the temperate-O + ashed subsoil had the same amount of nSOC as the temperate topsoil, it reacted in the same way as the O-horizons with no priming as a result of PyOM additions. However, nSOC in the subsoil did not show greater but lower priming than in the topsoil as a result of PyOM additions, despite the subsoil having a greater proportion of mineral-associated C as shown by lower DOC concentrations per unit C and a lower total C content (Table 2). This may be explained by the 5.5 times greater amount and 1.3 times greater proportion of DOC in the top- than the subsoil (Supplementary Table S1), which may have resulted in a larger proportion of nSOC be available for adsorption to PyOM surfaces (Whitman et al., 2014b) which was then unavailable to microorganisms (Supplementary Figure S1).

416 The negative priming caused by PyOM additions here therefore hinges primarily on the type of
417 organic matter and amount of DOC available. Largely microbial-derived nSOC with low C/N
418 ratios is more likely to be stabilized by adsorption than plant-derived nSOC with high C/N ratios
419 as was observed by Qiao et al. (2016). The greater negative priming by PyOM with sugar cane
420 additions (Keith et al., 2011) or after removal of some of easily mineralizable nSOC (Whitman et
421 al., 2014b) in contrast to our results of lower negative priming with litter nSOC and in the
422 subsoil may be explained by the lower nSOC contents in the cited studies of 0.5% and 1.1%,
423 respectively, in comparison to 5.3% in our topsoil. In addition, the C/N ratios of the added plant
424 litter by Keith et al. (2011) had a C/N ratio of 99 in comparison to 27-44 in our O horizons
425 (Table 2) suggesting different constraints on mineralization.

426 The lack of short-term positive priming observed here even in O horizons appears to be based on
427 a complex combination of mechanisms involved in how added PyOM affects nSOC
428 mineralization. This lack of positive priming in the studied boreal O-horizon stands in contrast to
429 interpretations from a litterbag experiment at the same site (Wardle et al., 2008). Even though
430 our study was conducted only over 90 d in comparison to 10 y for the litterbag experiment, the
431 only differences in nSOC disappearance in the latter were observed in the first six months. Since
432 our laboratory experiment was conducted at 30°C and optimum water conditions, and the
433 litterbag study under ambient temperature (mean annual temperature of 3.4°C) and likely non-
434 optimum soil moisture, the study periods may be comparable between the first six months in
435 Wardle et al. (2008) and the 90 d in our study. The reason for the apparent differences may be
436 that the litterbag experiment captures net losses from the bags, which included leaching losses,
437 whereas our incubation experiment only captured CO_2 evolution. Any DOC from the litterbags
438 in the O horizon may be adsorbed in the underlying mineral horizons (Lehmann and Sohi, 2008).

With additions of uncharred biomass, the subsoil with the most mineral associated (lowest nSOC content) and most decomposed (lowest C/N ratio) nSOC exhibited the largest short-term positive priming, potentially because the biomass additions were proportionally greater. Larger additions of uncharred biomass increased nSOC mineralization to a greater extent as shown for the boreal O-horizon. Co-metabolism or N limitation were unlikely to explain the increased nSOC mineralization in the subsoil, since C/N ratios were lowest in the subsoil (10.2), the added uncharred biomass had higher C/N ratios (31.6) and additions of metabolizable C may not increase mineralization of low-C/N (and thus more microbially processed) nSOC. More likely, desorption of nSOC from mineral surfaces may have made adsorbed C available to microorganisms due to the large amounts of added biomass that augmented DOC by an additional 134% (173 mg DOC-C kg^{-1}) of DOC present in soil (127 mg DOC-C kg^{-1} soil; Supplementary Table S1). This desorbed soil DOC likely had lower C/N values than the added DOC from uncharred biomass, being more similar to total soil mentioned above. The fact that the proportion of added uncharred biomass-C in microbial biomass was with 90% highest in the subsoil (Fig. 3a), and the metabolic quotient was comparably high for nSOC (Supplementary Fig. S4), supports the interpretation that more nSOC that was easily mineralizable, was available with additions of uncharred biomass. PyOM additions, however, did not add sufficient DOC (3 mg DOC-C kg^{-1} or 2% of the DOC present) to change the amount of mineralizable nSOC even in the subsoil.

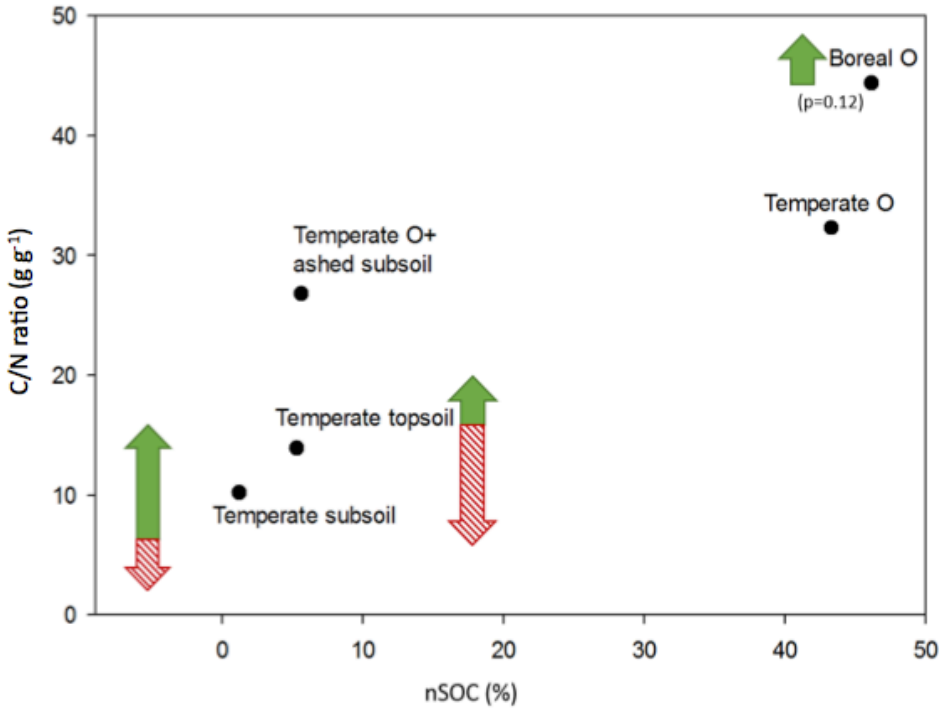

458

459 **Fig. 4.** Conceptual image of priming effects based on nSOC association with minerals (%) and degree of
460 microbial processing (C/N ratio). Green arrows indicate priming by biomass additions, red arrows
461 indicate priming by PyOM additions. Arrow direction indicates positive or negative priming, size
462 indicates approximate magnitude of priming effect ($p<0.05$).

463

464 **2.5. Conclusions**

465 This study showed significant short-term changes in nSOC mineralization as a result of additions
466 of charred or uncharred willow biomass, the direction and magnitude of which varied more with
467 nSOC properties for PyOM and more with application rate for uncharred biomass. The consistent
468 positive priming by equivalent additions of uncharred biomass additions and the consistent
469 negative priming in mineral soils with PyOM additions should be considered in evaluating the C
470 budget wherever PyOM input to soil occurs as a result of vegetation fires or deliberate additions
471 of biochar. Desorption of nSOC especially in subsoils was a likely explanation for the strong

positive priming induced by uncharred organic matter additions, rather than the commonly invoked co-metabolism. More attention should be paid to the form, not only the amount of nSOC for it is affected by priming, as well as the C/N ratio of the added substrate. Given the strong differences between organic and mineral horizons, investigations should be done with soils of different mineralogy or with constructed soils that vary only in their mineralogy. Additional studies with high measurement frequency will need to be conducted that assess whether the presence of plants and continuous C inputs will affect the short-term priming dynamics in both organic and mineral horizons.

Acknowledgements

This study was supported by the Carbon Cycles program of USDA-DOE (NIFA 2014-67003-22069) and the NSF-Basic Research for Enabling Agricultural Development program (BREAD grant number IOS-0965336). Any opinions, findings, conclusions, or recommendations expressed in this material are those of the authors and do not necessarily reflect the views of the donors.

References

Bingeman, C W, Varner J E, Martin W P. (1953) The effect of the addition of organic materials on the decomposition of an organic soil. *Soil Science Society of America Journal* 17: 34–38.

Black C, Evals D, White J, Ensminger L, Clark F. (1965) Methods of Soil Analysis Part 1: Physical and Mineralogical Properties, Including Statistics of Measurement and Sampling. *American Society of Agronomy* No. 9 in Agronomy Series. Madison, Wisconsin. pp 281

Blagodatskay E, Kuzyakov Y. (2008) Mechanisms of real and apparent priming effects and their dependence on soil microbial biomass and community structure: critical review. *Biology and Fertility of Soils* 45(2): 115-131.

Bruuslema T, Duxbury J. (1996) Simultaneous measurement of soil microbial nitrogen, carbon, and Carbon Isotope Ratio. *Soil Science Society of America Journal* 60: 1787-1791.

Chen J, Lui X, Zhang B, Lu H, Chi Z, Pan G, Li L, Zheng J, Zhang X, Wang J, Yu X. (2013) Biochar soil amendment increased bacterial but decreased fungal gene abundance with shifts in community structure in a slightly acid rice paddy from Southwest China. *Applied Soil Ecology* 71: 33-44.

Czimczik CI, Masiello CA. (2007) Controls on black carbon storage in soils. *Global Biogeochemical Cycles* 21.

Downie AE, Van Zwieten L, Smernik RJ, Morris S, Munroe PR. (2011) Terra Preta Australis: Reassessing the carbon storage capacity of temperate soils. *Agriculture, Ecosystems and Environment* 140: 137–147.

Eckmeier E, Egli M, Schmidt MWI, Schlumpf N, Nötzli M, Minikus-Stary N, Hagedorn F. (2010) Preservation of fire-derived carbon compounds and sorptive stabilization promote the accumulation of organic matter in black soils of the Southern Alps. *Geoderma* 159: 147-155.

Enders A, Hanley K, Whitman T, Joseph S, Lehmann J. (2012) Characterization of biochars to evaluate recalcitrance and agronomic performance. *Bioresource Technology* 114: 644-653.

Fontaine S, Bardoux G, Abbadie L, Mariotti A. (2004) Carbon input to soil may decrease soil carbon content. *Ecology Letters* 7: 314–320.

Keiluweit M, Nico PS, Johnson MG, Kleber M. (2010) Dynamic molecular structure of plant biomass-derived black carbon (biochar). *Environmental Science and Technology* 44:1247-1253.

Keith A, Singh B, Singh B P. (2011) Interactive priming of biochar and labile organic matter mineralization in a smectite-rich soil. *Environmental Science and Technology* 45: 9611–9618.

Kettler TA, Doran JW, Gilbert TL. (2001) Simplified Method for Soil Particle-Size Determination to Accompany Soil Quality Analysis. *Soil Science Society of Am*erica Journal 65:849-852.

Kögel-Knabner I, Zech W, Hatcher PG. (1988) Chemical composition of the organic matter in forest soils: the humus layer. *Journal of Plant Nutrition and Soil Science* 151(5): 331-340.

Kuzyakov Y, Friedel JK, Stahr K. (2000) Review of mechanisms and quantification of priming effects. *Soil Biology and Biochemistry* 32: 1485-1498.

Kuzyakov Y. (2010) Priming effects: Interactions between living and dead organic matter. *Soil Biology and Biochemistry* 42:1363-1371.

Kuzyakov Y, Friedel JK, Stahr K. (2000) Review of mechanisms and quantification of priming effects. *Soil Biology and Biochemistry* 32: 1485–1498.

Kuzyakov Y, Bol R. (2004) Using natural ^{13}C abundances to differentiate between three CO_2 sources during incubation of a grassland soil amended with slurry and sugar. *Journal of Plant Nutrition and Soil Science* 167: 669–677.

Laird DA. (2008) The charcoal vision; a win-win-win scenario for simultaneously producing bioenergy, permanently sequestering carbon, while improving soil and water quality. *Agronomy Journal* 100:178-181.

Lehmann J. (2007) A handful of carbon. *Nature* 447: 143-144.

Lehmann J, Sohi S. (2008) Comment on "Fire-Derived Charcoal Causes Loss of Forest Humus". *Science* 321: 1295.

Qiao N, Xu X, Hu Y, Blagodatskaya E, Lui Y, Schaefer D, Kuzyakov Y. (2016) Carbon and nitrogen additions induce distinct priming effects along an organic-matter decay continuum. *Scientific Reports* 6:19865.

Rumpel C, Eusterhues K, Kögel-Knabner I. (2004) Location and chemical composition of stabilized organic carbon in topsoil and subsoil horizons of two acid forest soils. *Soil Biology and Biochemistry* 36(1): 177-190.

Singh BP, Cowie A L, Smernik R. (2012) Biochar carbon stability in a clayey soil as a function of feedstock and pyrolysis temperature. *Environmental Science and Technology* 46: 11770–11778.

Sparks, Page A, Helmke P, Loeppert R. (1996) Methods of Soil Analysis Part 3—Chemical Methods. SSSA Book Ser. 5.3. SSSA, ASA, Madison, WI.

554 Vance ED, Brookes PC, Jenkinson DS. (1987) Microbial biomass measurements in forest soils:
555 the use of the chloroform fumigation-incubation method in strongly acid soils. *Soil Biology and*
556 *Biochemistry* 19: 697-702

557 Wang J, Xiong Z, Yan X, Kuzyakov Y. (2016) Carbon budget by priming in a biochar-amended
558 soil. *European Journal of Soil Biology* 76: 26-34.
559
560 Wardle DA, Nilsson MC, Zackrisson O. (2008) Fire-derived charcoal causes loss of forest
561 Humus. *Science* 320: 629–629.

562 Whitman T, Enders A, Lehmann J. (2014a) Pyrogenic carbon additions to soil counteract
563 positive priming of soil carbon mineralization by plants. *Soil Biology and Biochemistry.* 73: 33-
564 41.

565 Whitman T, Zhu Z, Lehmann J. (2014b) Carbon mineralizability determines interactive effects
566 on mineralization of pyrogenic organic matter and soil organic carbon. *Environmental Science*
567 *and Technology* 48: 13727–13734.

568 Whitman T, Zimmerman A, Bhupinder PS. (2015) Biochar for environmental Management.
569 Chapter 16: Priming effects in Biochar-amended soils: Implications of biochar soil organic
570 matter interactions for carbon storage. Second edition. Routledge, New York, NY.

571 Witt C, Gaunt J, Galicia C, Ottow J, Neue H. (2000) A rapid chloroform-fumigation extraction
572 method for measuring soil microbial biomass carbon and nitrogen in flooded rice soils. *Biology*
573 *and Fertility of Soils* 30: 510-519.

574 Zimmerman AR, Gao B, Ahn M-Y. (2011) Positive and negative carbon mineralization priming
575 effects among a variety of biochar-amended soils. *Soil Biology and Biochemistry* 43: 1169–1179.

576 Zimmerman AR, Ahn MY. (2010) Organo-mineral enzyme interactions and influence on soil
577 enzyme activity, in: Shukla G, Varma A (eds). *Soil Enzymology, Soil Biology,* Springer- Verlag,
578 Berlin Heidelberg, pp 271-292.

579
580
581
582
583
584
585
586
587

Supplementary Information

Priming of organic carbon in different soil horizons after additions of charred and uncharred organic matter

Silene DeCiucies[1], Thea Whitman[2], Dominic Woolf[1], Akio Enders[1], Johannes Lehmann[1,3]*

[1]Soil and Crop Sciences, School of Integrative Plant Science, Cornell University, Ithaca, NY 14850, USA

[2]Department of Soil Science, University of Wisconsin, Madison, WI 53706, USA

[3]Atkinson Center for a Sustainable Future, Cornell University, Ithaca, NY 149850

*Corresponding author, email: CL273@cornell.edu

Table of contents for supporting information

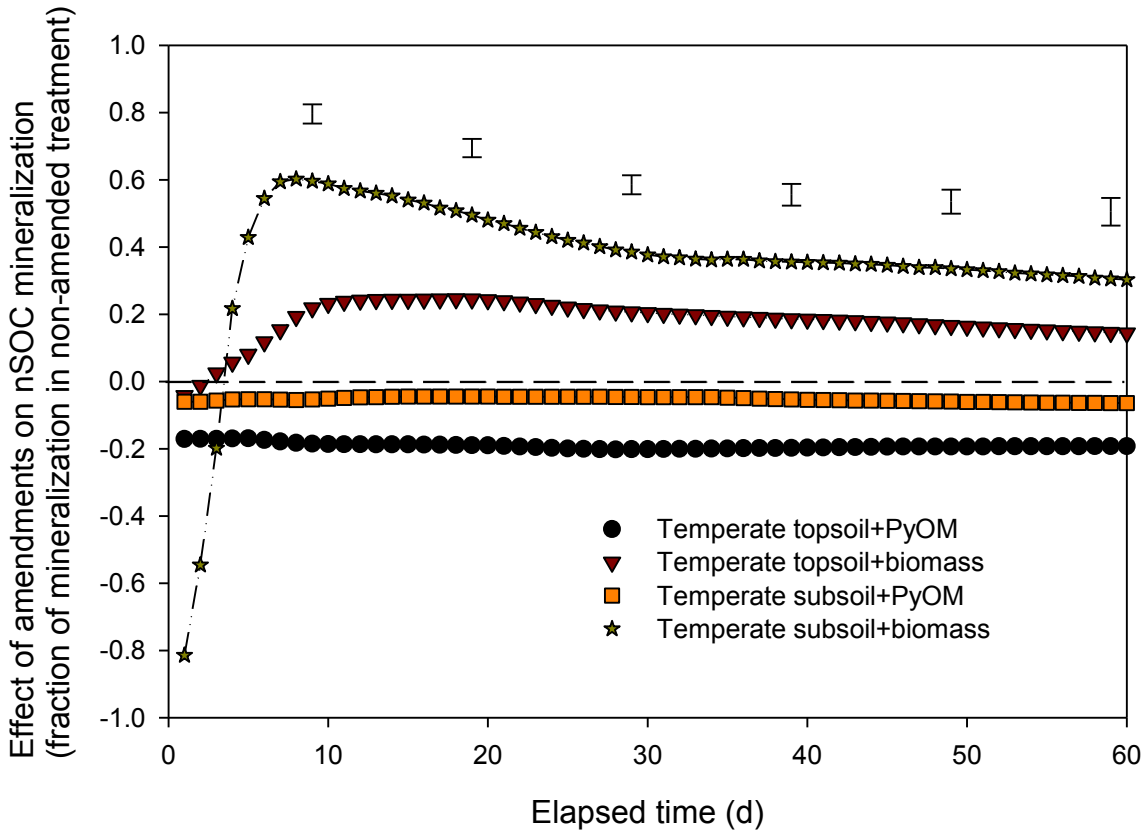

Supplementary Figure S1: Cumulative relative effect of PyOM additions on nSOC mineralization over time as a fraction of nSOC mineralized ($nSOC_{amendment} - nSOC_{unamended}$) / $nSOC_{unamended.}$). Dashed black line indicates unamended control; data above this line indicate positive priming, below indicate negative priming (n=4; bars show LSD at $p<0.05$).

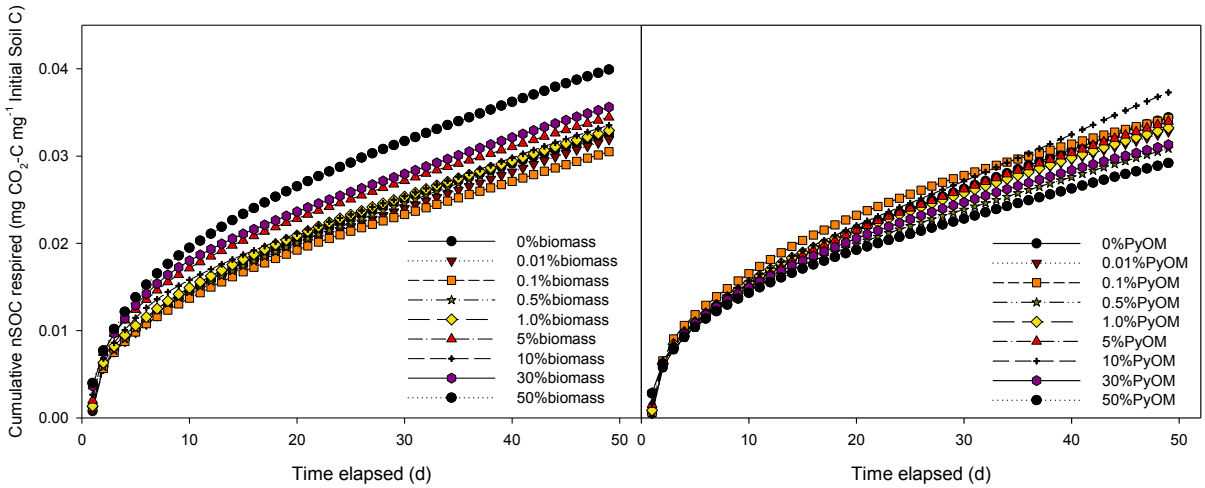

Supplementary Figure S2: Cumulative nSOC respiration per unit initial nSOC in boreal O-horizon with increasing application rates of uncharred biomass and PyOM. Left panel depicts biomass addition, and right panel depicts PyOM addition (n=1).

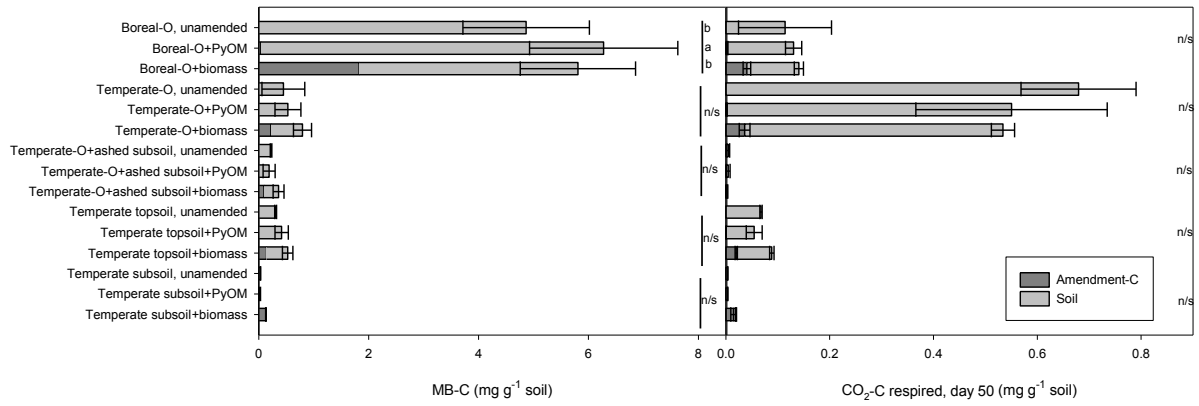

Supplementary Figure S3: Microbial biomass C (left panel) and cumulative C respired (right panel), from amendment (where applicable) and nSOC (means and standard errors; n=4).

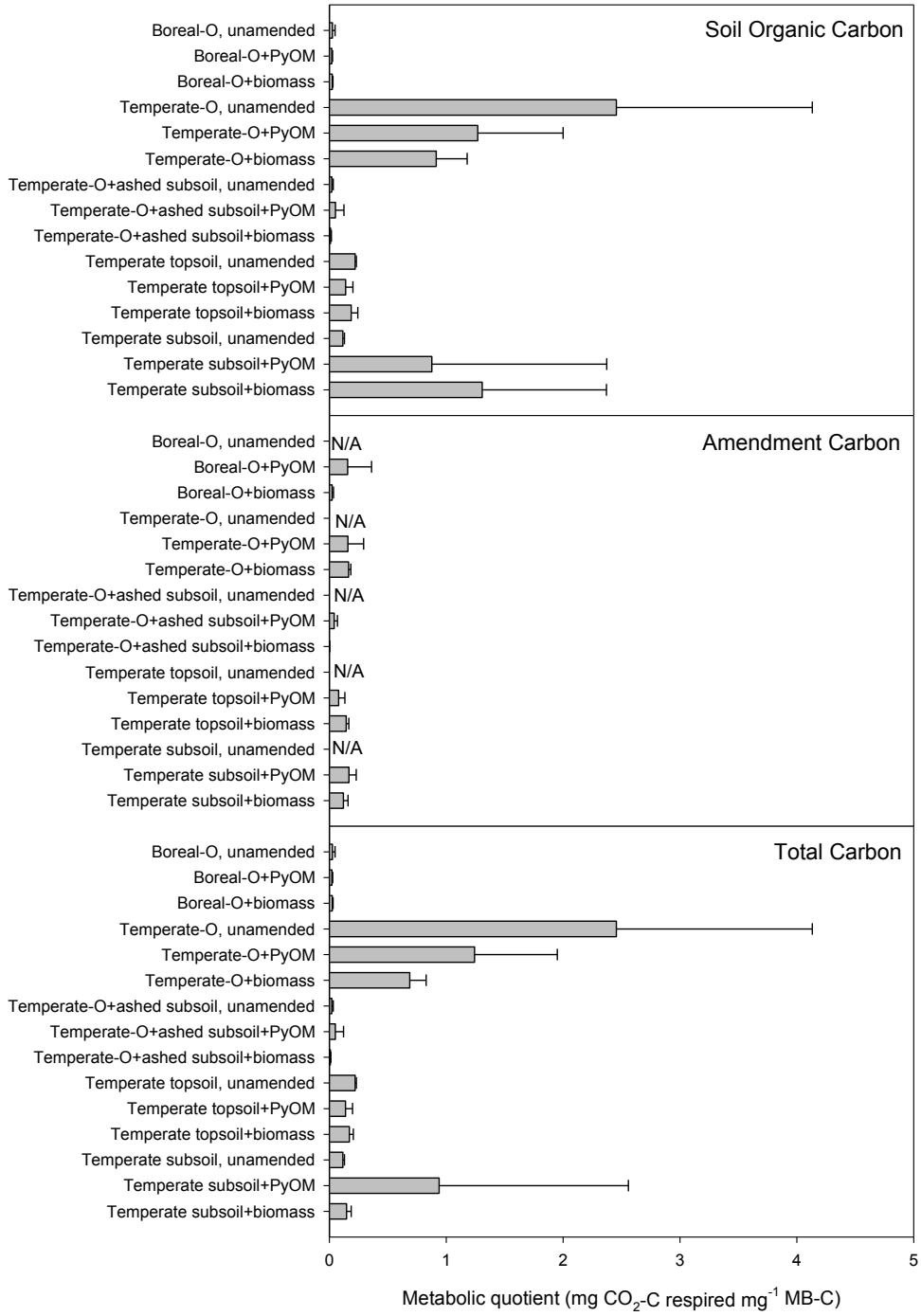

Supplementary Figure S4: Metabolic quotient of different soil horizons after incubation with uncharred biomass or PyOM. Metabolic quotient here refers to the total C respired divided by the MB-C and is used to describe the microbial efficiency of utilizing the C present (means and standard errors; n=4).

Supplementary Table S1. Amounts of C or DOC applied in comparison to nSOC and soil DOC.

Soil	Amendment	nSOC (mg C g^{-1} soil)	C applied (mg C g^{-1} soil)	Soil DOC (mg C kg^{-1} soil)	DOC applied (mg C kg^{-1} soil)
Boreal-O	PyOM	433	7.7	2965	2.8
Boreal-O	Biomass	433	16.8	2965	173.3
Temperate-O	PyOM	462	7.7	3742	2.8
Temperate-O	Biomass	462	16.8	3742	173.3
Temperate-O+subsoil	PyOM	56.2	7.7	384[a]	2.8
Temperate-O+subsoil	Biomass	56.2	16.8	384 [a]	173.3
Temperate topsoil	PyOM	52.8	7.7	703	2.8
Temperate topsoil	Biomass	52.8	16.8	703	173.3
Temperate subsoil	PyOM	12.2	7.7	127	2.8
Temperate subsoil	Biomass	12.2	16.8	127	173.3

[a] calculated value based on ashed subsoil and temperate-O data.

Supplementary Table S2. Microbial biomass and microbial quotient at the end of experiments (n=4).

Soil	Amendment	Microbial biomass (mg MB-C g^{-1} soil)	Microbial biomass from amendment (mg MB-C g^{-1} soil)	Total CO_2 respired[a] (mg CO_2-C g^{-1} soil day^{-1})	Metabolic quotient (mg CO_2-C g^{-1} MB-C day^{-1})
Boreal-O	Unamended	4.87	n/a	0.11	0.03
Boreal-O	PyOM	6.28	0.05	0.13	0.02
Boreal-O	Biomass	5.81	1.83	0.14	0.03
Temperate-O	Unamended	0.45	n/a	0.68	2.46
Temperate-O	PyOM	0.53	0.009	0.55	1.24
Temperate-O	Biomass	0.80	0.23	0.53	0.69
Temperate-O+subsoil	Unamended	0.22	n/a	0.005	0.02
Temperate-O+subsoil	PyOM	0.19	0.004	0.005	0.05
Temperate-O+subsoil	Biomass	0.36	0.09	0.003	0.01
Temperate topsoil	Unamended	0.31	n/a	0.07	0.22
Temperate topsoil	PyOM	0.42	0.01	0.05	0.14
Temperate topsoil	Biomass	0.53	0.142	0.09	0.17
Temperate subsoil	Unamended	0.03	n/a	0.003	0.12
Temperate subsoil	PyOM	0.02	0.001	0.003	0.94
Temperate subsoil	Biomass	0.13	0.13	0.02	0.15

n/a not applicable

[a]On the last day of the incubation when microbial biomass was extracted